

## Illinois State University ISU ReD: Research and eData

---

### Theses and Dissertations

---

6-5-2015

# Expression, localization, and kinetic characterization of the phospholipid biosynthesis enzyme CTP: phosphocholine cytidyltransferase from the protozoan parasite *Leishmania major*

Justin Daniel Theodore Lange  
*Illinois State University*, [jlange@ilstu.edu](mailto:jlange@ilstu.edu)

Follow this and additional works at: <https://ir.library.illinoisstate.edu/etd>

 Part of the [Biochemistry Commons](#), [Cell Biology Commons](#), and the [Parasitology Commons](#)

---

### Recommended Citation

Lange, Justin Daniel Theodore, "Expression, localization, and kinetic characterization of the phospholipid biosynthesis enzyme CTP: phosphocholine cytidyltransferase from the protozoan parasite *Leishmania major*" (2015). *Theses and Dissertations*. 451.  
<https://ir.library.illinoisstate.edu/etd/451>

This Thesis and Dissertation is brought to you for free and open access by ISU ReD: Research and eData. It has been accepted for inclusion in Theses and Dissertations by an authorized administrator of ISU ReD: Research and eData. For more information, please contact [ISUREd@ilstu.edu](mailto:ISUREd@ilstu.edu).

EXPRESSION, LOCALIZATION, AND KINETIC CHARACTERIZATION OF THE  
PHOSPHOLIPID BIOSYNTHESIS ENZYME CTP: PHOSPHOCHOLINE  
CYTIDYLYLTRANSFERASE FROM THE PROTOZOAN PARASITE  
*LEISHMANIA MAJOR*

Justin D.T. Lange

99 Pages

The eukaryotic parasite *Leishmania* is the causative agent of the disease leishmaniasis. *L. major* is the most common of 21 species that causes visceral leishmaniasis in humans, and 30 that cause the same disease in other mammals. Visceral leishmaniasis causes fever, weight loss, and over a short amount of time, multiple organ failure, and has a 100% mortality rate within 2 years. This makes it the second largest parasitic killer in the world behind malaria. Over 90% of the world's cases of visceral leishmaniasis have been reported in underdeveloped countries of India, Bangladesh, Nepal, Sudan, Ethiopia and Brazil, with 500,000 new cases being diagnosed worldwide each year. Nonetheless, the most popular drugs of choice for leishmaniasis treatment remain toxic, expensive, or subject to refractory infections.

Phospholipids used to construct biological membranes account for approximately 70% of total cellular lipid in *Leishmania*, and of that 30-40% is phosphatidylcholine (PC). PC is formed via the Kennedy pathways in *Leishmania*, as well as in many higher

eukaryotes, including mammals. The enzyme CTP: phosphocholine cytidyltransferase (CCT) catalyzes the addition of cytidine triphosphate (CTP) to phosphocholine yielding CDP-choline, a second, critical, rate limiting step in the formation of PC by the Kennedy pathway that has been shown to be reversibly membrane associated. Amino acid sequence analysis of CCT shows a high level of homology in the CCT catalytic region but a lack of the known carboxy terminal membrane-binding region in *L. infantum* and *L. major*. Thus, the nuclear localization signal, along with the classical carboxy terminal membrane binding domain is absent in these organisms and it is unknown whether CCT localizes to the nucleus, endoplasmic reticulum, or cytoplasm.

In investigation of the enzyme, the gene for *L. major* CCT has been tagged with a red fluorescent protein gene (mCherry) and successfully cloned into non-pathogenic *Leishmania tarentolae*. Confocal microscopy has revealed that *L. major* CCT is primarily cytoplasmic, while most likely also able to reversibly associate with internal membranes such as the endoplasmic reticulum and plasma membrane. CTP: phosphoethanolamine cytidyltransferase (ECT), an analogous enzyme of phosphatidylethanolamine (PE) synthesis, was also shown to be exclusively cytosolic using the same technique. In addition, a truncated mutant of *L. major* CCT containing the catalytic domain has been expressed in *Escherichia coli* and purified. *In vitro* assay of the enzyme yielded a maximal velocity ( $V_{max}$ ) of approximately 374 nmol/min/mg and substrate constant ( $K_m$ ) values of 0.0648 mM and 3.74 mM respectively for the substrates CTP and phosphocholine. The  $Mg^{2+}$  ion was used as a cofactor in the reaction, but the enzyme was also able to achieve maximal activity using  $Mn^{2+}$ ,  $Co^{2+}$ ,  $Ni^{2+}$ , and possibly  $Fe^{2+}$ . Additionally, the enzyme was most active at 37°C and pH 7.5. This summarizes

investigation of CCT as a possible therapeutic target for more efficacious treatment of leishmaniasis.

**KEYWORDS:** Cytidylyltransferase, *Leishmania*, Leishmaniasis, Phosphatidylcholine

EXPRESSION, LOCALIZATION, AND KINETIC CHARACTERIZATION OF THE  
PHOSPHOLIPID BIOSYNTHESIS ENZYME CTP: PHOSPHOCHOLINE  
CYTIDYLYLTRANSFERASE FROM THE PROTOZOAN PARASITE

*LEISHMANIA MAJOR*

JUSTIN D.T. LANGE

A Thesis Submitted in Partial  
Fulfillment of the Requirements  
for the Degree of

MASTER OF SCIENCE

School of Biological Sciences

ILLINOIS STATE UNIVERSITY

2015

Copyright 2015 Justin D. T. Lange

EXPRESSION, LOCALIZATION, AND KINETIC CHARACTERIZATION OF THE  
PHOSPHOLIPID BIOSYNTHESIS ENZYME CTP: PHOSPHOCHOLINE  
CYTIDYLYLTRANSFERASE FROM THE PROTOZOAN PARASITE

*LEISHMANIA MAJOR*

JUSTIN D.T. LANGE

COMMITTEE MEMBERS:

Jon A. Friesen, Chair

Kevin A. Edwards

Erik D. Larson

## ACKNOWLEDGMENTS

First and foremost, I would like to thank my Lord and Savior Jesus Christ for giving me the purpose and drive to complete this research, which I hope will be used by the scientific community for the betterment of the lives of his people. Next, I would like to thank Dr. Jon Friesen for his guidance and advice in this endeavor, which has allowed me to obtain meaningful results and become an independently thinking scientist. I would also like to thank my lab mates, past and present, especially Alisha Morganthaler, Ashley Boyd, Rose Stoller, Micheal Elsasser, and Jim Brault for making the lab a fun and friendly place to work, as well as helping me with experiments. Similarly, I would like to thank my co-workers in the Biology graduate school, including Pegan Sauls, Jay Pyle, Samantha Atkinson, Tony Martini, Sam MacFadden, Mike Krzyskowski, and Zach Smith, for being great comrades throughout the last three years. I would also like to thank my great friends outside of science, including John Cooper, Eric Meier, Alex Thoennes, Adam Leinhop, and Troy Lukas for providing me with the entertainment and support in the rest of my life to be able to keep things in perspective. Finally, I would like to thank my father and mother, Dr. Daniel and Linda Lange, and my sister, Sarah Lange, for the inspiration and support to drive all of my achievements in life.

J. D. T. L.



## CONTENTS

|   | Page    |
|---|---------|
| ACKNOWLEDGMENTS   | i       |
| CONTENTS  | ii      |
| TABLES  | iv      |
| FIGURES   | v       |
| CHAPTER   |         |
| I.    BACKGROUND AND INTRODUCTION   | 1       |
| Infection by <i>Leishmania</i> and Treatment of Leishmaniasis                                     | 1       |
| Membrane Composition in <i>Leishmania</i> , as well as Function and<br>Synthesis of Phospholipids | 7       |
| CTP: Glycerol-3-Phosphate Cytidylyltransferase as a Model<br>Enzyme                               | 14      |
| Structure and Function of CTP: Phosphocholine<br>Cytidylyltransferase                             | 17      |
| Structure and Function of CTP: Phosphoethanolamine<br>Cytidylyltransferase                        | 23      |
| Summary of Goals  | 25      |
| II.    EXPERIMENTAL METHODS   | E<br>27 |
| Amplification of <i>Leishmania</i> Genes by Polymerase Chain Reaction                             | 27      |
| Visualization of DNA using Agarose Gels   | 29      |
| Cloning of the Amplified <i>Leishmania</i> Genes into a Plasmid<br>Expression Vector              | 30      |
| Transformation of Competent <i>E. coli</i>  | 32      |
| DNA Sequencing of Inserted <i>Leishmania</i> Genes  | 33      |
| Low Temperature Protein Expression and Production   | 35      |
| Protein Purification using Immobilized Metal Affinity Chromatography                              | 37      |
| Determination of Protein Concentration by Method of Bradford                                      | 39      |

|  |        |
|--|--------|
| Sodium Dodecyl Sulfate Polyacrylamide Gel Electrophoresis  | 40     |
| Western Blot Immunoassay   | 41     |
| Determination of Enzyme Activity using Radioisotope Assay  | 42     |
| Determination of Kinetic Parameters and the Effects of Divalent Metal<br>Cations, Temperature, and pH on Enzyme Activity | 44     |
| Two-Step Cloning of the Amplified RFP and <i>Leishmania</i> Genes<br>Into a Plasmid Expression Vector                    | 45     |
| Growth and Transformation of <i>L. tarentolae</i> Cells  | 48     |
| Fixing and Staining of Cells for use in Confocal Microscopy  | 50     |
| <br>III. RESULTS AND DISCUSSION  | <br>51 |
| Putative LmCCT and LmECT Amino Acid Sequence Alignment<br>and Analysis   | 51     |
| Molecular Cloning of the Full Length and Truncated LmCCT<br>Genes into pET45b  | 58     |
| Purification of Truncated CCT  | 63     |
| Characterization of the Kinetic Properties of Truncated CCT  | 68     |
| Effect of Various Divalent Metal Cations on Truncated CCT<br>Activity  | 75     |
| Effect of pH and Temperature on Truncated CCT Activity   | 78     |
| Two-Step Cloning of the RFP Gene, followed by LmCCT and LmECT<br>Genes, into pLEXSY-sat2                                 | 81     |
| Cellular Localization of <i>Leishmania Major</i> CCT and ECT   | 86     |
| Conclusions and Future Work  | 90     |
| <br>REFERENCES   | <br>94 |

## TABLES

| Table  | Page |
|--|------|
| 1. Kinetics Experiment Primer Sequences and Restriction Sites.     | 27   |
| 2. Localization Experiment Primer Sequences and Restriction Sites. | 46   |
| 3. Purification of CCTrun by Metal Affinity Chromatography.        | 67   |
| 4. Kinetic Values of Various CCT Isoforms.                         | 74   |

## FIGURES

| Figure   | Page |
|--|------|
| 1. Regions Affected by Leishmaniasis.  | 1    |
| 2. Life Cycle of <i>Leishmania</i> .   | 3    |
| 3. Chemical Structure of Miltephosine.   | 5    |
| 4. The Kennedy Synthesis Pathway for Phosphatidylcholine.  | 10   |
| 5. Major Pathways of Phospholipid Synthesis in <i>Leishmania</i> .   | 13   |
| 6. Amino Acid Sequence Alignment of CCT, GCT, and ECT.   | 16   |
| 7. Functional Domains of CCT.  | 17   |
| 8. Three Dimensional Structure of Rat CCT236 $\alpha$ Bound with CDP-choline.                              | 19   |
| 9. Three Dimensional Structure of Rat CCT236 $\alpha$ Active Site.   | 20   |
| 10. Plasmid Map of pET-45b.  | 30   |
| 11. Plasmid Map of pLEXSY-sat2.  | 45   |
| 12. Amino Acid Sequence Alignment of CCT Isoforms.   | 52   |
| 13. Hydropathy Plot of <i>L. major</i> CCT.  | 54   |
| 14. Amino Acid Sequence Alignment of ECT Isoforms.   | 56   |
| 15. Hydropathy Plot of <i>L. major</i> ECT.  | 57   |
| 16. Agarose Gels of Amplified LmCCT and LmCCTtrun PCR Products.  | 58   |
| 17. Agarose Gels of Digestion of LmCCT and LmCCTtrun PCR products, as well as pET45b, with BamHI and XhoI. | 59   |
| 18. Agarose Gel of pET45b-LmCCT and pET45b-LmCCTtrun Redigest with BamHI and XhoI.                         | 61   |

|  |    |
|--|----|
| 19. Analysis of Full Length CCT Purification Fractions by SDS-PAGE and Western Blot.         | 64 |
| 20. Analysis of Truncated CCT Purification Fractions by SDS-PAGE and Western Blot.           | 66 |
| 21. Substrate Dependence Curves of CTP and Phosphocholine.                                   | 70 |
| 22. Lineweaver-Burk Plots for CTP and Phosphocholine.  | 72 |
| 23. Specific Activity of CCTtrun in the Presence of Various Divalent Cations.                | 76 |
| 24. Specific Activity of CCTtrun over a Range of pH.   | 79 |
| 25. Specific Activity of CCTtrun at 25 and 37°C.   | 80 |
| 26. Agarose Gels of Amplified mCherry PCR Product.   | 81 |
| 27. Agarose Gels of Digestion of mCherry PCR Product and pLEXSY-sat2 with BglII and KpnI.    | 82 |
| 28. Agarose Gel of pLEXSY-sat2-RFP Redigest with BglII and KpnI.                             | 83 |
| 29. Agarose Gels of Amplified LmCCT and LmECT PCR Product.                                   | 84 |
| 30. Agarose Gel of pLEXSY-sat2-RFP-CCT and pLEXSY-sat2-RFP-ECT Redigest with BglII and XbaI. | 85 |
| 31. Visualization of the mCherry Control by Confocal Microscopy.                             | 86 |
| 32. Visualization of CCT-mCherry by Confocal Microscopy.                                     | 88 |
| 33. Visualization of ECT-mCherry by Confocal Microscopy.                                     | 89 |

## CHAPTER I

### BACKGROUND AND INTRODUCTION

#### **Infection by *Leishmania* and Treatment of Leishmaniasis**

*Leishmania* is a protozoan parasite that is the causative agent of leishmaniasis, a disease which threatens 350 million people, mostly in third world countries. Over 90% of the world's cases of leishmaniasis have been reported in underdeveloped countries of India, Bangladesh, Nepal, Sudan, Ethiopia and Brazil, with 500,000 new cases being diagnosed worldwide each year (Figure 1; WHO, 2015).

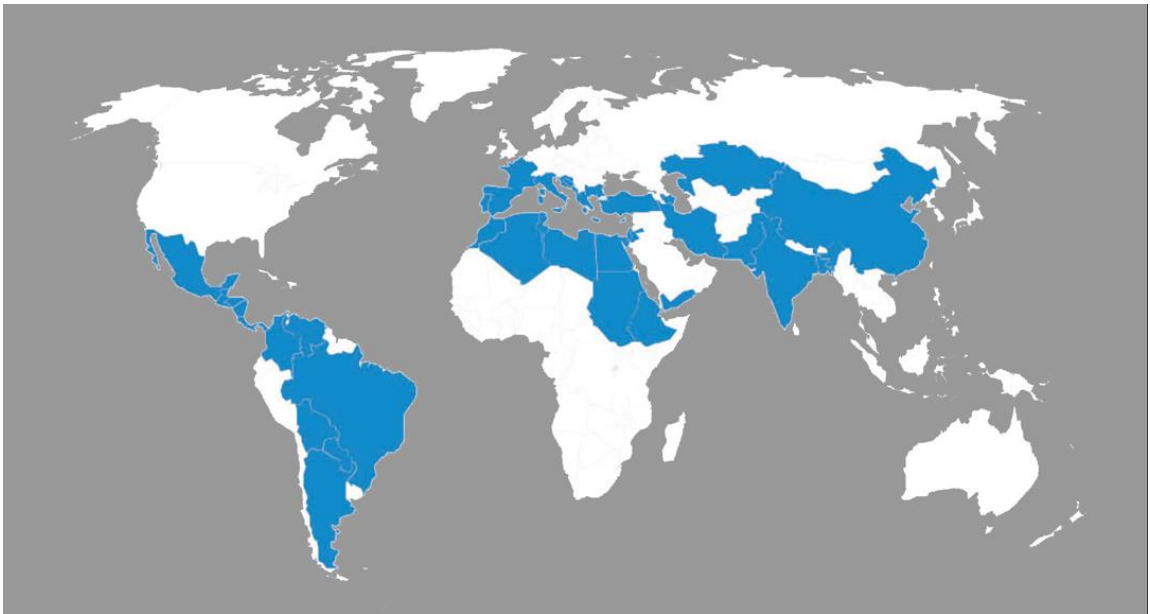


*Figure 1.* Regions Affected by Leishmaniasis. Countries affected by leishmaniasis are shaded in blue. Most are developing or undeveloped countries with tropical or sub-tropical climates.

There are also different forms of leishmaniasis including cutaneous, mucocutaneous, and visceral, which are caused by different species of *Leishmania*. Cutaneous leishmaniasis presents with disseminated and chronic skin lesions and is most commonly caused by *L. major*, *L. tropica*, and *L. aethiopica*. These open skin lesions may also become infected by opportunistic pathogens such as *Staphylococcus aureus*, which may make treatment even more difficult. Mucocutaneous leishmaniasis causes lesions that can partially or totally destroy the nasal, mouth, and throat mucosa, for which *L. braziliensis* is most often the culprit. Visceral leishmaniasis causes fever, weight loss, swelling of the spleen and liver, and anemia. *L. donovani* and *L. infantum* are responsible for this most debilitating form of the disease (Vannier-Santos et al., 2002). Over a short amount of time, the disease will cause multiple organ failure, and has a 100% mortality rate within 2 years. This makes it the second largest parasitic killer in the world behind malaria. Of particular concern is co-infection with the human immune-deficiency virus (HIV), as the two diseases are mutually reinforcing. HIV-infected people are particularly vulnerable to visceral leishmaniasis, while visceral leishmaniasis accelerates HIV replication and progression to acquired immuno-deficiency syndrome (AIDS) (WHO, 2015; CDC, 2015).

*Leishmania* is transferred between organisms by the sand flies of the genus *Phlebotomus* in the Old World (Southern Europe, North Africa, the Middle East, and South Asia) and *Lutzomyia* in the New World (Central and South America). *Leishmania* exist in two life-cycle stages: promastigote and amastigote. Promastigotes are extracellular, motile, and generally 5-20  $\mu\text{m}$  in length and 1-4  $\mu\text{m}$  in width, with an anterior flagellum that usually matches the size of their cell body. Amastigotes are

intracellular, nonmotile, ovular in shape, and usually 2  $\mu\text{m}$  in length and 1-4  $\mu\text{m}$  in width. Both contain a central nucleus and kinetoplast that lies anterior (Vannier-Santos et al., 2002). The life cycle of *Leishmania* starts when an infected sandfly takes a blood meal and injects the promastigote stage *Leishmania* into the host. The promastigotes are then internalized by phagocytic cells, such as macrophages, where the promastigotes transform into amastigotes. The amastigotes then multiply and spread to other phagocytic cells. When a sandfly takes a blood meal from this host, it will ingest the macrophages containing the amastigotes. These amastigotes will be converted back into promastigotes within the gut of the sandfly. The promastigotes then travel to the proboscis of the sandfly, where the cycle starts over (Figure 2; CDC, 2015).

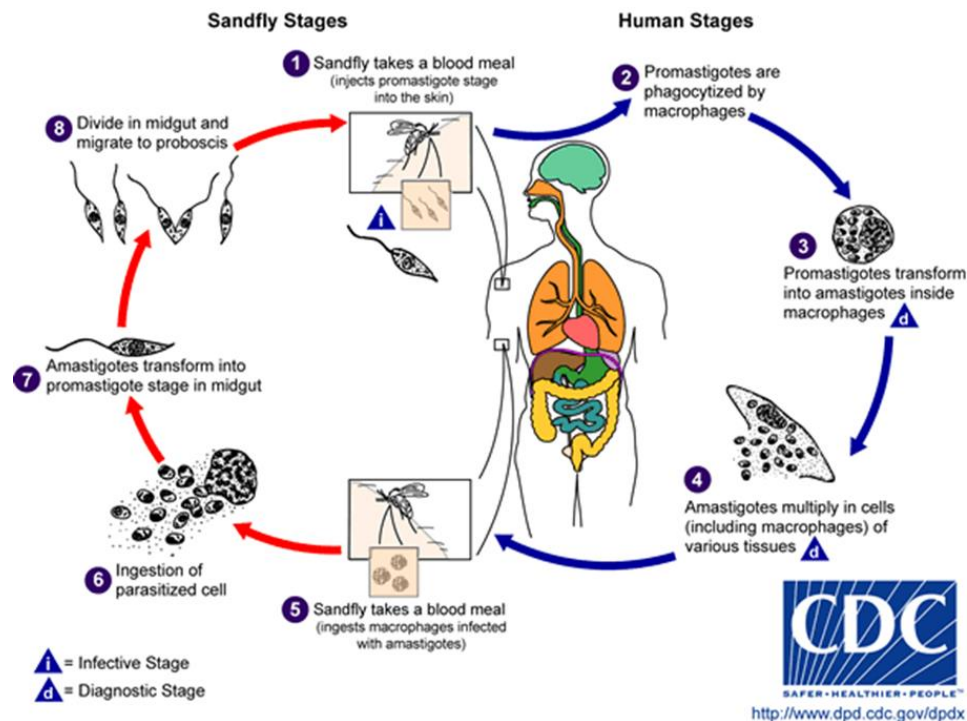


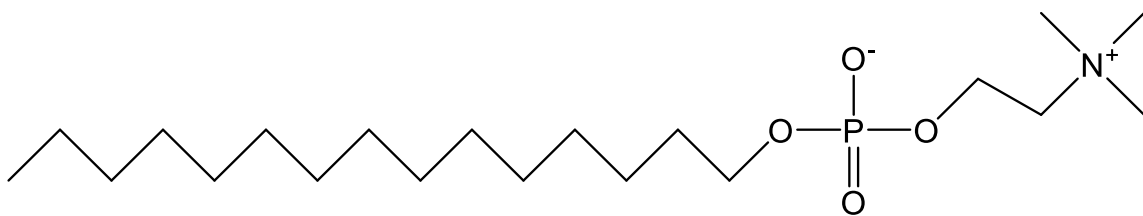
Figure 2. Life Cycle of *Leishmania*. The parasite alters between a promastigote and amastigote form in both the sandfly (primary host) and mammals (secondary host).



Several treatment options exist for leishmaniasis, but most are given in the form of injection. However, treatments given intravenously are not ideal for several reasons including multiple hospital visits, risk of HIV co-infection, and higher costs. Treatment options are also different for different species of *Leishmania*, different types of leishmaniasis, different regions of the world, and the health of the affected patient. The most common and effective intravenously administered drugs for leishmaniasis include the pentavalent antimony derivative drug sodium antimony gluconate (SAG), the antifungal drug amphotericin B, and the aminoglycoside paromomycin (Singh and Sivakumar, 2004). The mechanism for SAG is not fully known but it is generally thought to inhibit glycolytic enzymes and fatty acid oxidation in amastigotes. The side effects of SAG and other antimony derived drugs include pancreatitis, nausea, abdominal pain, nerve damage, and reduction of white and red blood cells as well as platelets. Resistance for this drug was first seen in the 1970s, but it still remains one of the primary drugs in the treatment against leishmaniasis due to its low cost (Singh and Sivakumar, 2004). Amphotericin B is an antifungal antibiotic that attaches to ergosterol in cell membranes, the major sterol in fungus and *Leishmania* which is not found in humans. Once attached, the drug prevents membrane synthesis from occurring and therefore causes the development of holes in the cell membrane and eventually cell death. It has been discovered that this drug attaches to cholesterol in mammalian cell membranes, which may cause such side effects as fever, chills, bone pain, and in rare cases cardiac arrest, reduction of potassium levels, and kidney toxicity. New liposomal formulations of amphotericin B have been made to reduce toxicity, however the cost of these new drugs limits them to severe cases of leishmaniasis or drug resistant strains of *Leishmania* only

(Singh and Sivakumar, 2004). Paromomycin is an aminoglycoside antibiotic that binds to 16S ribosomal RNA and in turn blocks protein synthesis. This is also often used in combination with antimonial compounds in treatment of severe cutaneous leishmaniasis. Side effects of paromomycin often include toxicity of the kidneys and vestibulocochlear nerve (Singh and Sivakumar, 2004).

Several oral drugs such as pentamidine, imidazole derivatives, and miltefosine are also used. Pentamidine was the first drug used in patients that had become refractory to pentavalent antimonials. Its mechanism of action includes blocking replication and transcription in the kinetoplast mitochondria. Accordingly, this drug causes a wide range of deleterious side effects, including diabetic symptoms, liver enzyme abnormalities, bone marrow effects like leukopenia and anemia, renal toxicity, and heart problems such as arrhythmia, hypotension, and heart failure (Singh and Sivakumar, 2004). The most effective has been the phosphocholine analogue compound miltefosine which was originally developed as an antineoplastic tumor drug (Figure 3).



Miltefosine

*Figure 3.* Chemical Structure of Miltefosine. Miltefosine, or 2-(hexadecyloxy-oxidophosphoryl) oxyethyl-trimethyl-azanium, is a phosphocholine analogue.

Much like its original purpose, miltefosine is thought to interact with protein kinase C in the plasma membrane of *Leishmania* which inhibits proliferation, alters

phospholipid and sterol composition, and activates cellular immunity. The drug has proven successful in clinical trials and is well tolerated, although low incidences of gastrointestinal disturbances and renal toxicity have been seen with treatment. However, a few species of *Leishmania* have showed resistance to miltefosine as early as 2003.

Overall, the drugs available for treatment of leishmaniasis are either very costly, have severe side effects, or certain *Leishmania* species are becoming resistant towards them (Singh and Sivakumar, 2004). Therefore, research is still needed in order to find additional pharmaceuticals and their targets for the treatment of this disease. The phospholipid synthesis enzyme CTP: phosphocholine cytidyltransferase (CCT) presents itself as an attractive potential drug target. This enzyme is involved in the synthesis of phosphatidylcholine (PC), a key phospholipid found in the cell membrane of *Leishmania*. PC represents about 30-40% of total cellular lipids in *Leishmania*, and a decrease below 25% has been shown to be extremely deleterious to the parasite cell (Zhang and Beverley, 2010). As a result, inhibition of CCT would not only disrupt membrane stability and vesicular trafficking, but may also cause abnormal signaling concerning cell growth, reproduction, and death.

## **Membrane Composition in *Leishmania*, as well as Function and Synthesis of Phospholipids**

Phospholipid synthesis is of extreme importance in all cells, including the organism of study, *L. major*. Phospholipids are comprised of a polar “head group”, glycerophosphoric acid, and connected fatty-acyl chains. These include phosphatidylcholine (PC), phosphatidylethanolamine (PE), phosphatidylserine (PS), phosphatidylinositol (PI), and phosphatidic acid (PA). The diversity of phospholipids is extensive, which includes having one or two fatty acyl chains, the length, branching, and double bond nature, or saturation, of those chains, and modification of the head group including phosphorylation and glycosylation. PC in *Leishmania* typically exists in 1,2 diacyl and 1-lyso-2 acyl forms consisting of unusually long and unsaturated fatty acyl species (Zufferey, 2003). While not extensively studied, it is thought that the polyunsaturated nature of PC in *Leishmania* most likely influences membrane fluidity by reducing its melting point and contributes to resistance against host-derived oxidative stress (Zhang and Beverley, 2010).

Phospholipids are the predominant lipid component comprising cell membranes of eukaryotic and prokaryotic cells and, in addition to their structural role in bilayer formation and membrane physiology, are also important for cell signaling. PI often serves as the precursor for signaling molecules found in most eukaryotic organisms including inositol 1,4,5-triphosphate, 1,2 diacylglycerol, arachidonic acid, lysophospholipids, and phosphatidic acid. PI may also be phosphorylated at different hydroxyl groups on the inositol moiety to form various bioactive phosphoinositides which regulate membrane trafficking and cytoskeleton remodeling in *Leishmania* (Coppolino et

al., 2002). In addition, *Leishmania* promastigotes, as well as other protozoan parasites, have been known to expose a large concentration of PS on the extracellular leaflet of their plasma membrane upon entry into the mammalian bloodstream. This PS exposure is also a sign given by apoptotic cells that phagocytic cells, such as macrophages, use to recognize and remove them. It has been hypothesized that *Leishmania* cells mimic this tactic in order to gain entrance into macrophages in a “Trojan horse” like manner (Wanderley et al., 2006). While signaling functions specific to PC have not yet been identified in *Leishmania*, the presence of phospholipases specific to PC that generate signaling molecules such as diacylglycerol, phosphatidic acid, and free fatty acids has been shown in other organisms. These often regulate and are regulated by protein kinase C and may control intracellular levels of  $Ca^{2+}$  (Barnett et al., 1993).

In terms of concentration, two of the major phospholipids in eukaryotes are PE and PC, with PC often the most abundant in these cells. However, membrane composition between organisms, tissues, and even individual cells often varies. Human endothelial cell phospholipid composition has been studied and PC is the most abundant phospholipid representing 36.6% of the total phospholipids, with PE representing 10.2%, and PS making up another 7.1% (Murphy et al., 1992). Yeast also contains PC in highest abundance with *Saccharomyces cerevisiae* having a phospholipid composition of 42% PC, 25% PE, 15% PI, 7% PS, and 9% cardiolipin (Kaneko et al., 1976). Protozoan parasites such as *Trypanosoma brucei*, *Trypanosoma cruzi*, *Leishmania*, and *Plasmodium*, in general contain about 40-50% PC, 35-45% PE, 4-11% PI, and less than 5% PS. Of particular interest, the membranes of *L. major* typically contain 33% PC, 10% PE, 10% PI, and 7% other phospholipids (Zhang and Beverley, 2010).

There are two possible phospholipid synthesis pathways that may be employed by organisms: a “salvage” pathway and the Kennedy, or *de novo*, synthesis pathway. In the salvage pathway, cytidine triphosphate (CTP) is first reacted with phosphatidic acid to form the product cytidine diphosphate-diacylglycerol (CDP-DAG) by CDP-DAG synthase. This reaction activates the phosphodiester bond for attack by the hydroxyl group located on a specific head group including either choline, ethanolamine, serine, inositol, or glycerol, which is used by a specific synthase enzyme to yield PC, PE, PS, PI, or PG (Aktas et al., 2010). The salvage pathway seems to be extensively used by prokaryotes and as yet no putative genes involved in this immediate pathway have been identified in *Leishmania*.

The Kennedy pathway differs from the salvage pathway in that CDP is first attached to the head group, not the DAG. The head group is first phosphorylated and then acts as a nucleophile which attacks the alpha-phosphate of CTP creating a CDP-head group. The hydroxyl group on DAG can then act as nucleophile and attack the alpha-phosphate of the CDP-head group to form the specific phospholipid. The only phospholipids synthesized via the Kennedy pathway are PC and PE (Kennedy and Weiss, 1956). As previously stated, the Kennedy pathway involves three enzymatic steps in the formation of PC. The first enzyme, choline kinase (CK), is soluble and phosphorylates choline to phosphocholine using adenosine triphosphate (ATP) as a phosphate donor, yielding adenosine diphosphate (ADP) as byproduct. The second enzyme and topic of this study, CTP: phosphocholine cytidyltransferase (CCT), catalyzes the addition of cytidine triphosphate (CTP) to phosphocholine, yielding CDP-choline and inorganic pyrophosphate byproduct. CCT has been shown to be reversibly membrane associated

and controls the critical, rate limiting step in the formation of PC by the Kennedy pathway. The third enzyme, choline phosphotransferase (CPT) catalyzes the addition of DAG to CDP-choline to form PC and cytosine monophosphate (CMP) as a byproduct, and is an integral membrane protein (Kent, 1997) (Figures 4, 5).

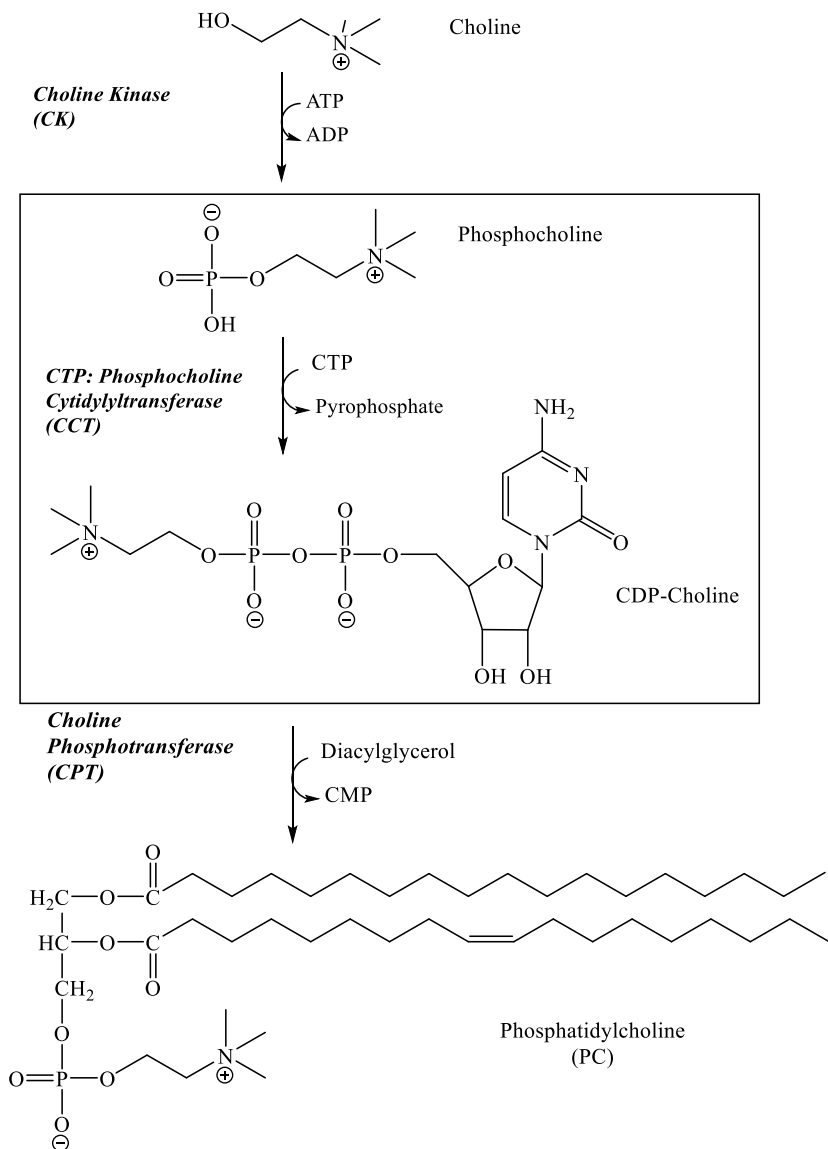


Figure 4. The Kennedy Synthesis Pathway for Phosphatidylcholine. The enzyme of interest to this work is CCT, which catalyzes the second reaction in this pathway.

Synthesis of PE is accomplished in a very similar fashion by using ethanolamine kinase (EK) and CTP: phosphoethanolamine cytidylyltransferase (ECT) which are typically cytosolic, and ethanolamine phosphotransferase (EPT) which is integrally membrane bound (Figure 5). However, many organisms express dual function choline/ethanolamine kinases (C/EK) and/or phosphotransferases (C/EPT), while cytidylyltransferases are always specific (Gibellini and Smith, 2010). The Kennedy pathway is used by eukaryotes and putative genes for C/EK, CCT, ECT, and C/EPT have been identified in *Leishmania* (Rogers et al., 2011). Of greatest concern, *L. major* CCT has been experimentally characterized in this study and provides its main focus, while *L. major* ECT has been characterized by a previous member of the lab and will be examined to a much lesser extent (Morganthaler, 2014).

However, more recent research has characterized an alternative route found in many eukaryotes which provides metabolites for PE synthesis in *Leishmania*. In this pathway, sphingolipids such as sphingosine-1-phosphate (S-1-P) and dihydrosphingosine-1-phosphate (DHS-1-P) are degraded by sphingosine-1-phosphate lyase (SPL) to produce phosphoethanolamine and *trans*-2-hexadecanal, the former of which is then utilized in the reaction catalyzed by ECT in *de novo* PE synthesis (Figure 5; Zhang et al., 2007). The drastic decrease of PE content and disappearance of PC in double mutants lacking serine palmitoyltransferase (SPT) (*spt2*<sup>-</sup>), a sphingolipid synthesis enzyme, or sphingosine 1-phosphate lyase (*spl*<sup>-</sup>), suggests that this is a major component of PE synthesis pathway in *Leishmania* promastigotes. Addition of ethanolamine restored the wild type phenotype, indicating *L. major* promastigotes are unable to produce significant amounts of these critical phospholipids without sphingolipids. However, *L.*



*major* *spt2<sup>-</sup> spl<sup>-</sup>* amastigotes remain phenotypically normal and infective, as well as both SPT2 and SPL mRNA/proteins are down regulated in wild type amastigotes, indicating that amastigotes most likely synthesize PE using ethanolamine from other metabolic routes (Zhang et al., 2007). Additionally, a putative gene for phosphatidylserine decarboxylase (PSD), which converts PS into PE by removing carbon dioxide from the serine head group, has also been found in *Leishmania* (Figure 5; Rogers et al., 2011). PSD is typically an integral membrane protein and is found in most other eukaryotes (Schuiki and Daum, 2009).

Finally, any available PE, whether formed via the Kennedy pathway, breakdown of sphingolipids, or decarboxylation of PS, can be converted into PC by the enzyme phosphatidylethanolamine methyltransferase (PEMT) (Figure 5). One or multiple PEMT enzymes catalyze the transfer of three successive methyl groups to the ethanolamine head group of PE to form PC, using *S*-adenosyl methionine as a methyl group donor (Vance, 2014). PEMT is found in most eukaryotes and two PEMT enzymes, PEM1 and PEM2, have very recently been experimentally characterized in *L. major*. *In vitro* enzyme assays using protein purified from recombinant *Leishmania* showed expression and activity were highest in mid-log growth stage promastigotes and lowest in macrophage cell-invasive amastigotes. Identification of an endoplasmic reticulum (ER) retention amino acid sequence, as well as studies using *in vivo* immunofluorescence and fractionation with the detergent Digitonin, indicated that both PEMT enzymes are integral membrane proteins that localize to the ER. Analysis of cellular lipids using electrospray ionization tandem mass spectrometry from a variety of recombinant mutant *S. cerevisiae* yeast strains showed that expression of *Leishmania* PEM1 and PEM2 rescued a phenotype in which

exogenous choline was required in yeast double null mutants. These experiments were also used to show the extent to which each PEMT enzyme catalyzes each successive methylation reaction. PEM1 forms monomethyl-phosphatidylethanolamine (MMPE) and dimethyl-phosphatidylethanolamine (DMPE), while PEM2 forms DMPE and PC (Figure 5). Finally, it was shown that both PEMT enzymes were inhibited by several choline analogs including miltefosine (Bibis et al., 2014).

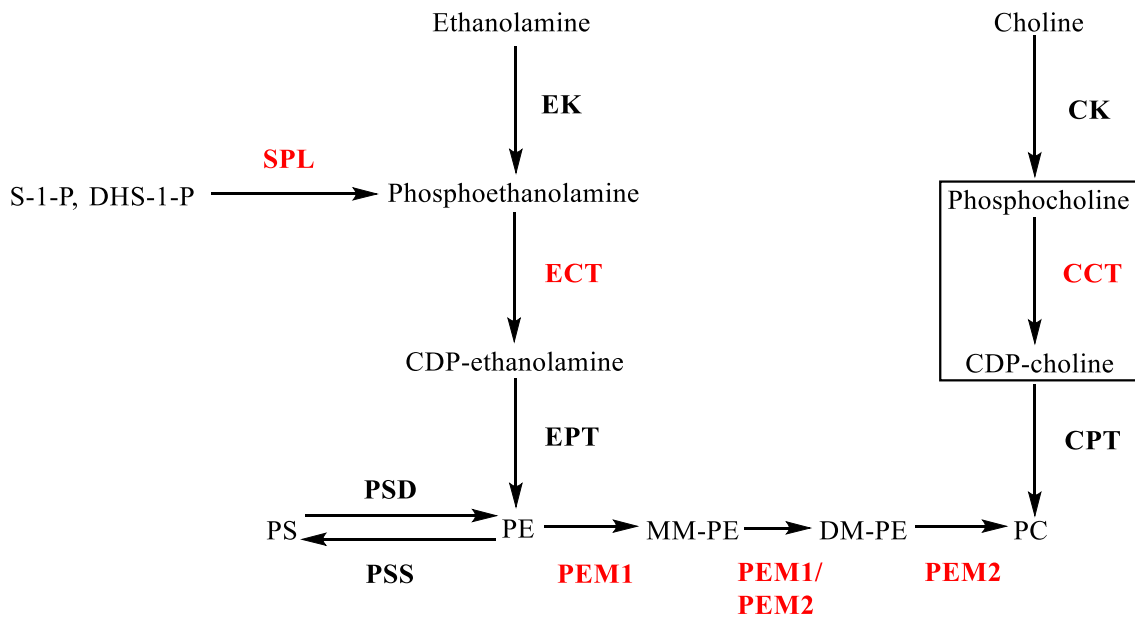


*Figure 5.* Major Pathways of Phospholipid Synthesis in *Leishmania*. This flow chart shows the major routes for synthesis of PC, PE, and PS in *Leishmania*. Putative enzymes of which candidate genes have been identified in the *Leishmania* genome, but not characterized, are shown in black, while enzymes that have been experimentally characterized are shown in red.

### **CTP: Glycerol-3-Phosphate Cytidylyltransferase as a Model Enzyme**

The cytidylyltransferase family describes a group of enzymes that utilize CTP as a substrate to attach to another substrate with a free hydroxyl group. CTP: glycerol 3-phosphate cytidylyltransferase (GCT) from the bacterium *Bacillus subtilis* is the best characterized member of the cytidylyltransferase family. GCT catalyzes the addition of CTP to glycerol-3-phosphate to yield CDP-glycerol and inorganic pyrophosphate as byproduct. CDP-glycerol is eventually converted to teichoic acid, a polysaccharide needed for synthesis of gram positive bacterial cell walls (Park et al., 1993). GCT is, on average, the smallest enzyme of the cytidylyltransferase family, with *B. subtilis* GCT having just 129 amino acids and a molecular mass of 28 kDa (Weber et al., 1999). Due to its small structure, GCT has become the model enzyme for studying the structure and function of cytidylyltransferases, including CCT and ECT. Amino acid sequence alignment of GCT, CCT, and ECT indicates the members of the cytidylyltransferase family have two highly conserved amino acid sequences, denoted HxGH and RTxGxST, that are believed to be necessary for catalysis (Figure 6; Weber et al., 1999, Fong et al., 2006, Lee et al., 2009). *In vitro* enzyme assay of site directed mutants showed that H14A and H17A, found in the HxGH region, as well as D11A, D38A, R55A, D66A, H84A, and D94A all but eliminated the activity of the enzyme compared to wild type. Also, R113A, T114A, S118A, and T119A, found in the RTxGxST region, all decreased GCT activity to less than 10% of wild type level (Park et al., 1997).

The three dimensional crystal structure of *B. subtilis* GCT was the first in the cytidylyltransferase family to be solved. These initial GCT crystal structures have provided a glimpse into the relationship between structure and catalysis, as GCT was

observed to be a dimer wherein each monomer folds into a single globular catalytic domain containing five alpha helices and five beta sheets (Weber et al., 1999). Additionally, crystal structures showing *B. subtilis* GCT bound to CDP-glycerol product have identified T9, F10, H17, K44, K46, W95, and R113 as critical active site amino acids (Figure 6; Pattridge et al., 2003). All of these active site residues have either identical or functionally similar counterparts found in the same three-dimensional orientation in the crystal structure of the catalytic domain of rat CCT bound to CDP-choline product (Figure 9; Lee et al., 2009).

```

RatCCT   1  MDAQSSAKVNSRKRKREKVPKPGNGATEEDGIPSKVQRCVGLRQPAPFSDE
BsGCT    1  -----
RatECT    1  -----

RatCCT   51  IEVDFSKPYVRVTMEEACRGTPCERPVRVYADGIFDLFHS■GHARALMQAK■
BsGCT    1  -----MKKVITYGTFDLLHWGHIKLLERAK■
RatECT    1  ----MIRNGHGAGGAAGLKGPGGQRTVRVWCDG■YDMVHY■HSNQLRQAR■

RatCCT  101  NIFPNTYLVGVCSDELTHNFKGFTVMNENERYDAVQHC■RYVDEV■WRNAP■
BsGCT   26  QL--GDYLVVAISTDEFNLQK■KKAYHSYEH■RKLI■LETIRYVDEVIPEKN■
RatECT   47  AM--GDYLVGVH■DEEIAKHKGPPVFTQEE■YKMQA■IKV■DEVVPAAP■

RatCCT  151  WILTPEFLAE■HRIDFVAHDDIPYSSAGSDDVYKH■KEAGMFAPTQRTEGI■
BsGCT   74  WEQKKQDIIDHNIDVFVMGDDWEGKDFD-----LKDQCEVVYLPRTTEGI■
RatECT   95  YVTTLLETLDK■HNCD■FCVHGNDITLTVDGRD■TYEEV■KQAGRYRECKRTQGV■

RatCCT  201  STSDIITRVRDYDVYARR-NLQRGYTAKELNVSFINEK■KYHLQERV■DKV■
BsGCT  118  STTKIKEEAGL-----
RatECT  145  STIDL■VGRMLLVTKAHHSSQEMSSEYR--EYAD■SFGK■P--PHPT■PAGDTL■

RatCCT  250  KKKVKDVEEKSKEFVQKVEEKSIDLIQKWEKSR-----
BsGCT  -----
RatECT  191  SS-----EVSSQCPGGQSPWTGVSQFLQTSQKIIQFASGKE

RatCCT  284  -----EFIGSFLEMFGPEGALKHMLKEGKGRMLQAI■SPK-----
BsGCT  -----
RatECT  227  PQPGETVIYVAGAFDLF-----HIGHVDFLQEVHKLAKR■PYVIAG■

RatCCT  318  -----QSPSSSP■HERSPSP-----SFRWPFS-----
BsGCT  -----
RatECT  267  LHFDQEVNRYKGNYPIM-NLHERT■LSVLACRYVSEVVIGAPYSV■TAELL■

RatCCT  340  -----GKTS-----PSSSPASLSRCKAVTC■DIS■EDEED-----
BsGCT  -----
RatECT  316  NHFKVDLVCHGKTEIVPDRDGS■DPYEEP■KRRGIFC■QIDSGSD■LT■TDLIVQ■

```

Figure 6. Amino Acid Sequence Alignment of CCT, GCT, and ECT. Rat CCT (accession NP\_511177), *B. subtilis* GCT (accession AAB27724), and Rat ECT (accession NP\_446020) are aligned using Clustal Omega and BoxShade programs. Amino acids highlighted in grey represent those that are similar, and those highlighted in black are identical. Also, amino acids highlighted in blue are active site amino acids identified from crystal structures, and those highlighted in red are known to be necessary for catalysis.

## Structure and Function of CCT: Phosphocholine Cytidylyltransferase

CCT catalyzes the addition of cytidine triphosphate (CTP) to phosphocholine, yielding CDP-choline and inorganic pyrophosphate byproduct (Figure 4, 5). CCT is the most extensively studied of the cytidylyltransferase enzymes and has been characterized from a variety of organisms including human, rat, the yeast *S. cerevisiae*, the model plant *Arabidopsis thaliana*, the fly *Drosophila melanogaster*, the nematode *Caenorhabditis elegans*, and the protozoan *Plasmodium falciparum* (Kalmar et al., 1994; Friesen et al., 1999; Friesen, Park, and Kent, 2001; Helmink and Friesen, 2004; Tilley et al., 2008; Friesen, Liu, and Kent, 2001; Yeo et al., 1997). Past studies using amino acid sequence alignment, mutagenesis, and enzyme-specific proteolysis have indicated that there are three main functional regions within CCT isoforms; an amino terminal catalytic domain, a membrane binding region, and a phosphorylated carboxy terminal domain (Figure 7; Kent, 1997).

```
MDAQSSAKVNSSKRRKEVPGPNGATEEDGIPSKVQRCVGLRQPAPFSDEIEVDFSKPYVRVTMEEACRG
TPCERPVRVYADGIFDLFHSGHARALMQAKNLFNTYLVGVCSDELTHNFKGFTVMNENERYDAVQHCR
YVDEVVRNAPWTLTPEFLAEHRIDFVAHDDIPYSSAGSDDVYKHIKEAGMFAPTQRTREGISTSDIITRIV
RDYDVYARRNLQRGYTAKELNVSFINEKKYHLQERVDKVKKKVKDVEEKSKEFVQKVEEKSIDLIQWEE
KSREFIGSFLEMFGPEGALKHMLKEGKGRMLQAISPKQSPSSSPTHERSPSPSFRWPFSGKTSSPSSPAS
LSRCKAVTCDISEDEED
```

*Figure 7.* Functional Domains of CCT. Amino acid sequence of rat CCT $\alpha$  showing a possible nuclear localization signal highlighted in blue, the catalytic domain highlighted in green, the membrane binding domain highlighted in yellow, and phosphorylation domain highlighted in purple.

The catalytic domain of CCT contains the highly conserved HxGH and RTxGxST regions in primary sequence. While considering the previously discussed mutations of

GCT to inform relationship between structure and function in CCT, K122 and R196 were identified as important functional residues in rat CCT (Figure 6, 9). In this study, three mutant enzymes were assayed; K122A, K122R, and R196K. K122A only maintained 0.30% wild-type activity while K122R only retained 0.09% wild-type activity. Also, both lysine mutants showed significant increases in  $K_m$  values with respect to phosphocholine, which led to the conclusion that K122 is involved in the coordination of phosphocholine within the active site. Kinetic assays of R196K revealed 24% retention of wild-type activity while the  $K_m$  for CTP was 30 times higher. This study, coupled with structural information from the crystallization of GCT bound to CTP, indicated that R196 is involved in the coordination of CTP. In summary, these findings lead to the conclusion that K122 and R196 both play a significant role in the substrate binding process by providing necessary charge and steric stabilization (Helmink et al., 2003). This was proven when the crystal structure of the truncated, nuclear isoform CCT $\alpha$  from the rat *Rattus norvegicus* was solved. Analysis showed a globular dimeric structure, with each monomer containing six alpha helices and five beta sheets (Figure 8).

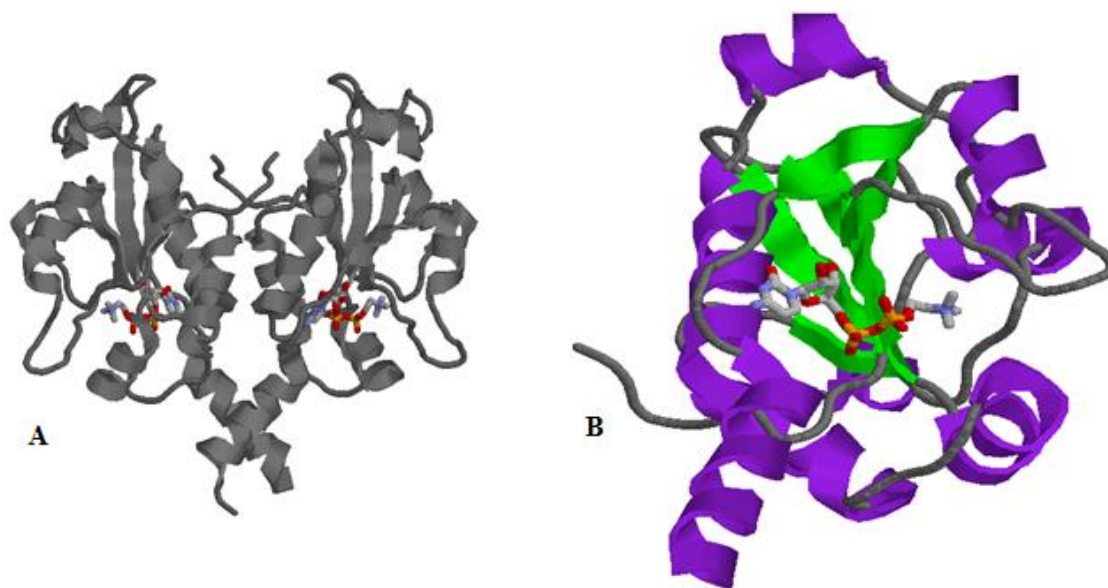


*Figure 8.* Three Dimensional Structure of Rat CCT236 $\alpha$  Bound with CDP-choline. (A) Frontal view orientation of homodimer, shown in gray, bound with CDP-choline, shown in CPK colors. (B) Right side view of monomer, with  $\alpha$  helices shown in purple and  $\beta$  sheets shown in green. Bound CDP-choline shown in CPK colors. Both images constructed using PDB 3HL4 coordinate file in Rasmol.

In the CCT $\alpha$  monomer, amino acids 1-236 comprise the catalytic domain, 237-314 are the membrane binding region, and 315-367 makes up the phosphorylated domain (Figure 7). The truncated version of rat CCT $\alpha$ , named CCT236, contained only the first 236 amino acids (the catalytic domain) due to limited solubility caused by the membrane binding domain in aqueous solution. As previously alluded to in GCT, the three-dimensional structure of rat CCT236 bound to CDP-choline has identified I84, F85, H92, K122, H168, Y173, and R196 as critical active site residues (Figure 9; Lee et al., 2009).



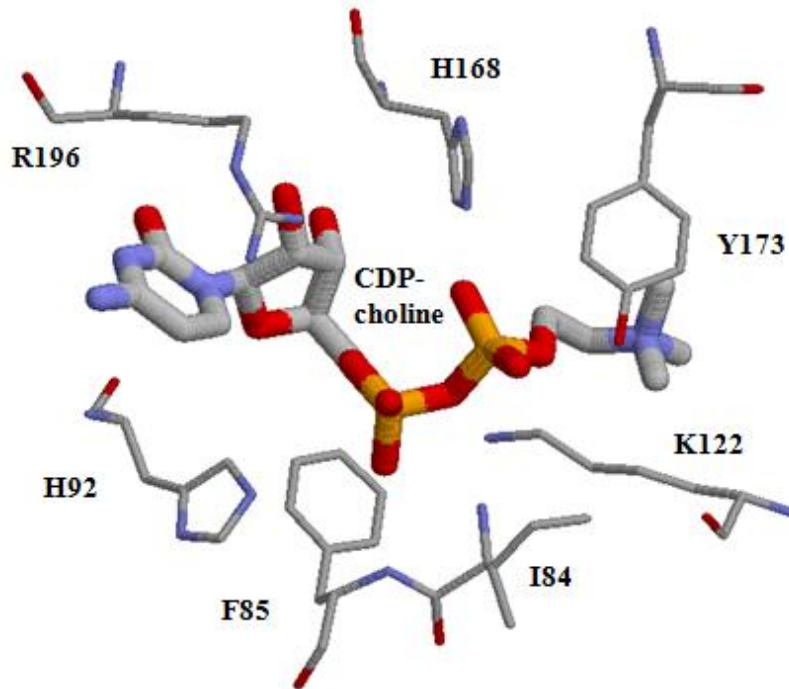


*Figure 9.* Three Dimensional Structure of Rat CCT236 $\alpha$  Active Site. Structures shown in CPK colors with critical active site residues shown in smaller thickness and bound CDP-choline product shown in greater thickness. Interaction distances between atoms are scaled proportionally.

The membrane binding domain of CCT is responsible for regulating its activity through reversible association with membranes. While known to contain a large concentration of hydrophobic amino acids and perform the same function in mammals, yeast, *C. elegans*, and *P. falciparum*, the primary amino acid sequence identity is not highly conserved. Central to this regulatory function is the property that mammalian CCT is present as both a soluble and a membrane-associated form within the cell, as shown by protein purification. In isolation, the membrane binding domains from rat and *C. elegans* have little secondary structure, based on circular dichroism analysis, but form an alpha helix upon membrane binding (Friesen, Liu, and Kent, 2001). Synthetic peptides

identical to the membrane binding domain from rat and *P. falciparum* show a similar transformation induced by membrane binding (Larvor et al., 2003). The formation of this amphipathic alpha helix activates the enzyme and increases the rate of PC synthesis. For example, in the absence of lipids, the full-length rat CCT $\alpha$  was shown to have very low catalytic efficiency and a  $K_m$  value for CTP that is 100 times higher than the average cellular concentration. Binding to anionic lipids significantly increases the catalytic efficiency and lowers the  $K_m$  value for CTP (Ding et al., 2012).

Experiments with rat and *C. elegans* CCT isoforms identified the membrane binding domain amino acids and postulated that it is responsible for inhibition of the enzyme. *C. elegans* CCT was truncated after amino acids 319, 281, 266, 245, or 225. Comparison of these five truncations to full-length wild-type CCT in the presence of PC vesicles containing the fatty acid oleate (1:1 PC:oleate) showed that the two shortest proteins were maximally active regardless of the amount of lipid available. Thus, it was concluded the CCT245 and CCT225 are both truncated before the membrane binding domain. The fact that CCT245 activity was not dependent on lipid availability, unlike CCT266, suggested that the amino acids between 246 and 266 were involved in the activation of the enzyme through association with the lipids of a cell membrane (Friesen, Liu, and Kent, 2001).

A more recent study utilized site directed mutagenesis to find which individual amino acids in this region were responsible for membrane binding. L246S, W249S, I256S, I257S, and F260S mutants demonstrated low activity in the absence of lipid vesicles, similar to wild-type CCT. However, lipid stimulated activity was markedly reduced compared to wild-type. Mutational analysis of F260 implicated this

residue as a contributor to auto-inhibition of CCT due to activity of the F260S mutant being higher than wild type in the absence of lipid vesicles. Mutation of L246, W249, I256, and I257 simultaneously to serine resulted in significantly higher activity compared to wild type in the absence of lipid vesicles and an enzyme that was not lipid activated, implicating the entire region as being auto-inhibitory in aqueous solution (Braker et al., 2009). It is largely unknown whether this region contributes to auto-inhibition in the absence of membrane lipids is due to a lack of structural rearrangement or actual binding interaction with the catalytic site. Nonetheless, a very recent study in rat CCT $\alpha$  has shown that as much as 100 times amount of membrane binding peptide compared to a catalytic truncation was not able to decrease activity in the absence of lipids, suggesting the lack of a strong interaction with the catalytic domain (Ding et al., 2012).

The presence of a nuclear localization signal (RKRRK) on the amino terminal side of the catalytic region is found in CCT isoforms that localize to the nucleus, including mammalian CCT $\alpha$  (Wang et al., 1995). However, recent studies have revealed the presence of another isoform of CCT in mammals, denoted CCT $\beta$ . CCT $\alpha$  was shown to be located in the nucleus while CCT $\beta$  was determined to be a cytosolic isoform using immunofluorescence (Lykidis et al., 1998). *D. melanogaster* also contains two CCT isoforms, CCT1 and CCT2, which have been recently characterized by a past member of the laboratory. Intracellular visualization of each CCT isoform was accomplished by confocal microscopy using carboxy-terminal green fluorescent fusion proteins and CCT1 was shown to be located in the nucleus, while CCT2 was cytosolic (Tilley et al., 2008).

## **Structure and Function of CTP: Phosphoethanolamine Cytidylyltransferase**

ECT catalyzes the addition of cytidine triphosphate (CTP) to phosphoethanolamine, yielding CDP-choline and inorganic pyrophosphate byproduct. ECT has not been studied as extensively as CCT, as concentration of PE in most eukaryotic cell membranes is much less than PC (Murphy et al., 1992; Kaneko et al., 1976; Zhang and Beverley, 2010). Analysis of amino acid sequences of ECT from human, rat, and yeast reveals a significant difference in the domain structure of the enzyme in comparison to CCT and GCT. It has been observed that CCT and GCT isoforms have a single HxGH site and, therefore, a single active site per polypeptide chain, while ECT isoforms have two HxGH sites. This observation suggests ECT may have two catalytic domains within a single polypeptide. Despite the duplication of the HxGH site, ECT isoforms typically have just one complete RTxGxST site in the amino terminal half of the sequence, leading to the possibility that the carboxy terminal half of the protein may not contain a fully functional catalytic site. Also, the carboxy terminal end of typical ECT isoforms does not appear to have the same membrane binding domain as found in CCT (Bladergroen et al., 1999).

Additionally, older studies using centrifugation of liver homogenates and cDNA from rat liver cells determined that ECT and CCT activity were separate, and that, unlike CCT, the ECT isoform from this organism was entirely cytosolic and not regulated by addition of exogenous lipids *in vitro* (Vermueulen et al., 1993). An isoform of ECT from bloodstream *Trypanosoma brucei*, a parasite closely related to *Leishmania*, has also very recently been characterized. Studies using immunofluorescence showed that *T. brucei* ECT, much like the mammalian isoform, localized to the cytosol (Gibellini et al., 2009).

However, studies in *Chlamydomonas reinhardtii*, a single-celled green algae, provide a less complex view of PE metabolism as PC and PS are not present in this organism. Analysis of amino acid sequence alignment with isoforms from rat, human, and yeast show that *C. reinhardtii* ECT contains a unique amino terminal sequence of 50 amino acids not found in the other isoforms. This amino terminal sequence contains a subcellular localization sequence for mitochondrial targeting, as well as significant hydrophobicity, and the capability to form an amphipathic  $\alpha$ -helix. Differential centrifugation and comparison with known marker enzymes showed that *C. reinhardtii* ECT is bound to the outer membrane of the mitochondria (Yang et al., 2004). Similarly, an ECT isoform from the castor bean *Ricinus communis* L endosperm was also shown to localize to the mitochondria, as well as be slightly activated by a mixture of phospholipids (Wang and Moore, 1991). These results indicate that ECT localization between the cytosol and mitochondria may be a difference between mammalian (or residing therein) and photosynthetic organisms.

## Summary of Goals

CCT is an attractive potential drug target for leishmaniasis due its regulatory activity in the *de novo* synthesis of phosphatidylcholine in the Kennedy pathway (Figure 4). This is strengthened by the hypothesis that the Kennedy pathway may be the predominant route for PC synthesis in infective amastigotes, as PEMT activity in these cells is nearly non-existent and the *Leishmania* cell would have a wealth of access to choline within the mammalian host (Bibis et al., 2014). Characterizing the biochemical properties of the enzyme from *L. major* is the first step of understanding how CCT functions. First, recombinant DNA encoding the CCT protein from *L. major* will be cloned into *E. coli* cells and the protein will be produced by inducible expression. Purification of the protein will be accomplished using affinity column chromatography and a series of isolating washes. Purified CCT enzyme will then be used to catalyze the addition of CTP and [<sup>14</sup>C] phosphocholine to form [<sup>14</sup>C]CDP-choline, which will be isolated and quantified in a radioisotope scintillation assay. Assay of varying concentrations of CTP and [<sup>14</sup>C] phosphocholine will determine the maximal velocity ( $V_{max}$ ) and substrate constant ( $K_m$ ) for each substrate, while CCT activity will also be assessed in the presence of various divalent metal cations, and at different temperature and pH. The work performed will hopefully provide the scientific community with a better understanding of the properties of the *Leishmania* CCT, so that in the future more specific pharmaceuticals and effective dose regimes can be designed to treat leishmaniasis by inhibiting this enzyme.

Also, amino acid sequencing will be used to identify critical catalytic residues and possible membrane binding domains in CCT. The gene for CCT will be recombinantly

expressed with mCherry red fluorescent protein (RFP) as a fusion protein construct in non pathogenic *L. tarentolae*. Subcellular localization of the mCherry tagged fusion protein will then be visualized using confocal microscopy. This will determine the intracellular localization of *Leishmania* CCT which is currently unknown, although other isoforms have been individually shown to localize to the nucleus and throughout the cytosol (Wang et al., 1995; Lykidis et al., 1998; Tilley et al., 2008). Also mentioned previously, an isoform of ECT from *L. major* has been characterized by a previous member of the lab in an unpublished study (Morganthaler, 2014). This work mostly identifies its kinetic parameters and activity in the presence of various divalent metal cations. Although previous studies in other organisms suggest the cytosol and or mitochondria as probable targets, ECT localization within the *Leishmania* cell remains undetermined (Vermueulen et al., 1993; Gibellini et al., 2009; Yang et al., 2004; Wang and Moore, 1991). Knowledge of the subcellular localization of both CCT and ECT in *Leishmania* promastigotes would not only provide insight into organelle specific allocation of PC or PE synthesized by the Kennedy pathway, but would also yield information useful in synthesis of an inhibitors that might be used as a possible therapeutic for leishmaniasis.

## CHAPTER II

### EXPERIMENTAL METHODS

#### **Amplification of *Leishmania* Genes by Polymerase Chain Reaction**

The polymerase chain reaction (PCR) was used to amplify the full length gene encoding *Leishmania major* CCT (Genbank ID: XM\_001682490), a truncation after the 1267 bp position, the full length gene encoding *Leishmania major* ECT (Genbank ID: CAJ08605), and the RFP gene, mCherry. A PCR reaction mixture was made containing 5  $\mu$ L of 100  $\mu$ M forward and reverse single-stranded oligonucleotide primers (Sigma-Aldrich), flanking the 5' and 3' ends of the gene respectively, that were used to amplify the *L. major* enzyme genes from genomic DNA or the mCherry gene from a Hto-RFP plasmid (courtesy of Dr. Kevin Edwards, Illinois State University) (Table 1).

Table 1

#### *Kinetics Experiment Primer Sequences and Restriction Sites*

| Name     | Oligonucleotide Sequence                                      | Restriction Enzyme |
|----------|---|--------------------|
| LmCCT5   | 5'-ATCTA <u>GGATCCC</u> <u>ATG</u> CCGCATCTGCTT<br>GAGC-3'    | <u>BamHI</u>       |
| LmCCTtr5 | 5'-ATCTA <u>GGATCCC</u> <u>ATG</u> CTGGTGGACTTG<br>TCGTAC -3' | <u>BamHI</u>       |
| LmCCT3   | 5'-ATCTA <u>CTCGAGTCA</u> TGCCCCGTCCTTCACC-3'                 | <u>XhoI</u>        |

*Note.* Forward (5') and reverse (3') oligonucleotide primer sequences are listed. Start codons are noted in green and stop codons are noted red (reverse complement).



The mixture also contained 400  $\mu\text{L}$  of water, 15  $\mu\text{L}$  of 10 mM deoxynucleotide triphosphate (dNTP) mixture, 50  $\mu\text{L}$  of 10x *Pfx* amplification buffer, 25  $\mu\text{L}$  of 10x PCR<sub>x</sub> enhancer solution, and 1  $\mu\text{L}$  of Platinum® *Pfx* DNA polymerase (Invitrogen). Then, 96  $\mu\text{L}$  of the master mix was added to four separate tubes containing 1, 2, 4, and 8  $\mu\text{L}$  of 50 mM  $\text{MgSO}_4$ . These reaction tubes were amplified using a PTC-200 DNA Engine Thermal Cycler PCR on a cycle of three temperatures (94°C for 15 sec., 45°C for 30 sec., and 68°C for 1 min.) repeated 30 times. At 94°C the double-stranded template DNA denatures, the primers then anneal at 50°C, and at 68°C the thermostable *Pfx* DNA polymerase catalyzes the elongation of a new DNA strand by incorporating new dNTPs. Once PCR was completed, the amplified double-stranded DNA products were analyzed on a 0.7% (w/v) agarose gel, purified using a PureLink™ Quick PCR Purification Kit (Invitrogen), and stored at -20°C.

### **Visualization of DNA using Agarose Gels**

An agarose gel separates DNA fragments based on the length of nucleotides. Using a microwave oven, a mixture of 0.7% (w/v) agarose was heated in 0.5x TBE (44.5 mM Tris, 44.5 mM boric acid, 1 mM EDTA) until dissolved. SYBR safe (Invitrogen) was added to the hot mixture in a 5  $\mu$ L per 100 mL ratio. SYBR safe is a fluorescent molecule that intercalates into DNA and allows for the visualization of DNA when UV light strikes the gel. The warm mixture was placed into a plastic mold and allowed to cool to room temperature before use. DNA samples were prepared for analysis by adding 5  $\mu$ L of 5X loading buffer (Promega) to 20  $\mu$ L of each sample yielding a final concentration of 1x, which adequately allows for visualization of samples as they run towards the anode in the gel. Once the samples were prepared, they were loaded into the wells of the gel and the DNA fragments separated at 150 V for approximately 30 min. Gels were imaged using a Kodak Gel Logic 200 Imaging System.

## Cloning of the Amplified *Leishmania* Genes into a Plasmid Expression Vector

After the CCT, CCTtrun, and ECT genes were amplified, they were placed into two separate plasmid expression vectors. These plasmids contain several restriction enzyme sites in a multiple cloning site that are used to remove sections of the original plasmid and replace them with DNA amplified by PCR. The restriction enzyme sites utilized for the cloning of *L. major* CCT and CCTtrun into pET45b were BamHI and XhoI (New England Biolabs) (Table 1, Figure 10).

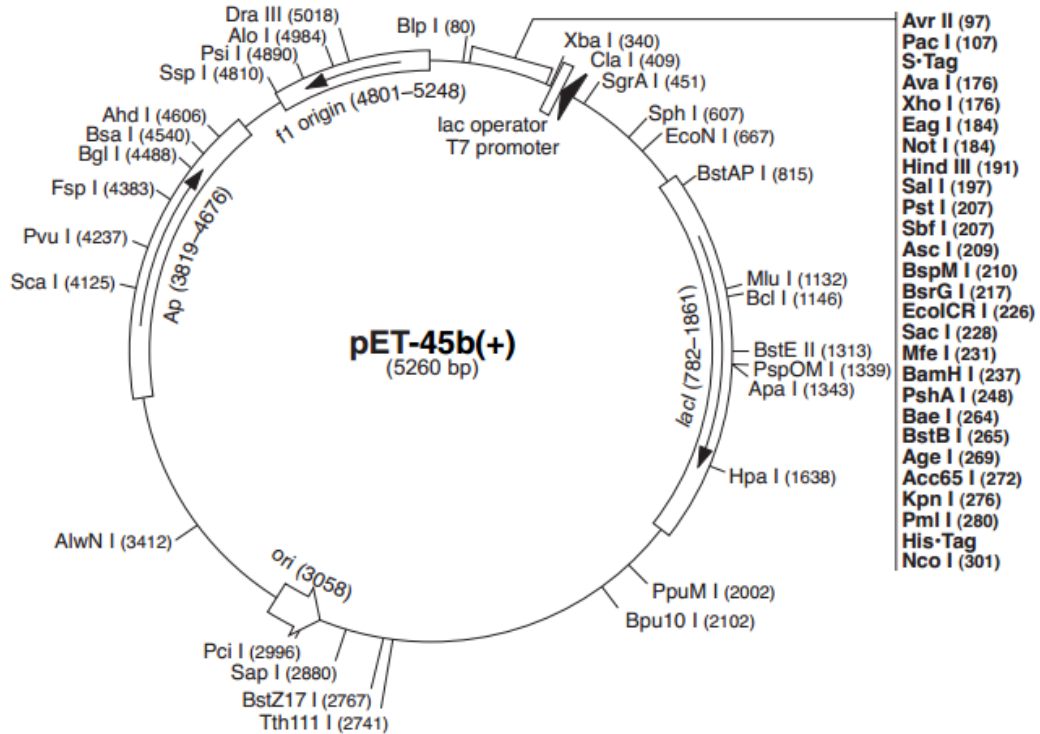


*Figure 10.* Plasmid Map of pET-45b. The BamHI (237) and XhoI (176) restriction sites within the multiple cloning site were used to clone the genes of interest. Upstream of the 5' cloning site is the 6x histidine tag (His Tag). The plasmid also contains an ampicillin antibiotic resistance gene.

A restriction digest was performed to cut the pET45b plasmid vector by incubating 5  $\mu$ L of pET45b, 2  $\mu$ L of 10x NEB buffer #2, 0.5  $\mu$ L of BamHI, 0.5  $\mu$ L of XhoI, and 12  $\mu$ L of water at 37°C overnight. Separate restriction digests were also performed to cut the PCR amplified CCT and CCTtrun gene insert fragments. Both the plasmid vector and insert DNA fragments were run on a 0.7% agarose gel, excised, and purified using the PureLink™ Quick Gel Extraction Kit (Invitrogen). The digested CCT and CCTtrun gene inserts were both separately ligated into pET45b by incubating 8.5  $\mu$ L of insert (CCT or CCT trun) with 8.5  $\mu$ L of pET45b plasmid vector, 2  $\mu$ L of 10x buffer with 10 mM ATP, and 1  $\mu$ L of T4 DNA ligase (New England Biolabs) at 15°C overnight.

### **Transformation of Competent *E. coli***

Transformation is a process in which plasmid DNA is taken up by competent bacterial cells. Separate mixtures of 50  $\mu$ L of *dam<sup>-</sup> dcm<sup>-</sup>* strain of *E. coli* cells (New England Biolabs) and 5  $\mu$ L of either pET45b-CCT or pET45b-CCTtrun plasmid DNA were incubated for 30 min. on ice. Next, the mixture was heat shocked for 1 min. at 37°C and placed on ice for 2 min. The mixture was then added to 1 mL of Luria Broth (LB) media and incubated at 37°C for 1 hr. The mixture was then plated on LB agar plates that contained 100  $\mu$ g/ml ampicillin and incubated at 37°C overnight in order to select for growth of transformed cells by way of the plasmid ampicillin resistance gene. A variety of colonies were selected from the plates and grown at 37°C overnight in LB media containing 100  $\mu$ g/ml ampicillin. The replicated plasmid DNA was then purified from the cell culture using a PureLink™ Quick Plasmid Miniprep Kit (Invitrogen). A small amount of the purified plasmid DNA was then digested with the restriction enzymes BamHI and XhoI as previously described. Finally, the resulting DNA fragments were analyzed using a 0.7% agarose gel to determine if the fragments matched the size of the inserted CCT and CCTtrun genes. Purified plasmid DNA that yielded correctly sized fragments was stored at -20°C.

### **DNA Sequencing of Inserted *Leishmania* Genes**

DNA sequencing was carried out using a kit obtained from Applied Biosystems. Sequencing of the LmCCT and LmCCTtrun genes utilized two primers, a T7 promoter primer (5'-TAATACGACTCACTATAGGG-3') that annealed upstream of the Bam HI site or a T7 terminator primer (5'-GCTAGTTATTGCTCAGCGG-3') that annealed downstream of the XhoI site. A sequencing reaction was prepared by mixing 2 µl of purified plasmid DNA with 1 µl Big Dye Terminator 5X buffer, 1 µl Big Dye Terminator Ready Mix® and 1 µl of 1 µM T7 forward promoter primer or 1 µM T7 terminator primer. The mixtures were placed in the thermal cycler and subjected to 25 cycles of 96°C for 10 sec., 50°C for 5 sec., and 60°C for 4 min. The contents of the PCR tubes were mixed with 25 µL of 95% ethanol, 1 µL 3 M sodium acetate pH 5 and 1 µL 125 mM EDTA. The samples were incubated at room temperature for 15 min. before being centrifuged at 16000 x g for 20 min. The supernatant liquid was removed and 35 µL of 70% ethanol was added to wash the DNA. The samples were vortexed for approximately 5 sec. and centrifuged for 5 min. at 16,000 x g. The wash liquid was removed and the samples were dried at 16,000 x g for 5 min. using a speedvac.

The dried DNA samples were analyzed using capillary electrophoresis on a 3130 Genetic Analyzer (Applied Biosystems®) operated by a technician in the School of Biological Sciences. The Ready Reaction Mix® contains a thermostable DNA polymerase, deoxynucleotides (dNTPs), and fluorescently labeled dideoxynucleotides (ddNTP). Each ddNTP emits a different color light when excited. When the polymerase attaches a ddNTP, the polymerization reaction comes to a stop. During the 25 cycles, the polymerase will attach a ddNTP at every nucleotide position in the gene under

investigation, giving rise to a ladder of DNA fragments varying in size by one nucleotide. Capillary electrophoresis separates these fragments based on size, and a laser excites the fluorescent dyes which emit a photon that is captured by a detector and transmitted to a monitor to create a chromatogram.

## Low Temperature Protein Expression and Production

The pET45b-LmCCT and pET45b-LmCCTtrun purified plasmid DNA was used to transform competent Arctic Express (DE3) RIL *E. coli* cells, as described previously, for production of recombinant full length and truncated *L. major* CCT protein. These cells were chosen after protein production using standard BL21 *E. coli* failed and cultivation of protein by lowering temperature, and subsequently expression level, was thought to be the solution.

The term “Arctic Express” arises from the fact that these cells contain a pACYC-based plasmid encoding the chaperonin proteins Cpn10 and Cpn60, as well as a gentamycin resistance gene. Cpn10 and Cpn60 are cold-adapted chaperonin proteins from the psychrophilic bacterium *Oleispira antarctica*, which facilitate the correct folding of proteins with significant hydrophobic character at lower temperatures between 4-12°C. DE3 denotes the *E. coli* contain a gene which expresses the T7 RNA polymerase from the *lacUV5* promoter upon induction by isopropyl-1-thio- $\beta$ -D-galactopyranoside (IPTG). This polymerase then binds to the T7 promoter on the pET45b vector and initiates RNA synthesis of the target gene. As their name implies, these cells also contain a pSC101-based plasmid cloned with extra copies of the *argU* (R), *ileY* (I), and *leuW* (L) tRNA genes, as well as a streptomycin resistance gene. These additional tRNAs facilitate expression of proteins encoded by rare codons in *E. coli* that are found more frequently in *Leishmania*.

Following transformation, these cells were plated on LB agar plates containing 100  $\mu$ g/ml ampicillin, to maintain the expression plasmid, and grown overnight at 37°C. A colony from the transformation plate was selected and added to 100 mL of LB broth



containing 100  $\mu\text{g}/\text{ml}$  of ampicillin and 20  $\mu\text{g}/\text{ml}$  of gentamycin, to maintain the chaperonin plasmid, and the cells were grown overnight in a 37°C incubator/shaker at 250 rpm. The following day, the cells were transferred into a flask with 1 L of LB media containing no selection antibiotics and grown for 3 hrs. at 30°C with 250 rpm shaking. The 1 L culture was then transferred to a hot plate in the cold room to incubate and stir. Once the culture equilibrated to 10-13°C, 100 mg IPTG (Sigma) was added to induce production of CCT and CCT trun protein. The cell culture was then allowed to grow for 72 hrs. Finally, the 1 L cell culture was split into 250 mL portions, harvested by centrifugation in an Avanti™ J-251 centrifuge (Beckman) at 5,000 rpm (4,650 x g) for 5 min., and stored at -20°C.

### **Protein Purification using Immobilized Metal Affinity Chromatography**

After growth of the cells expressing the enzyme, the cells were centrifuged and resuspended in 20 mL of lysis buffer containing 50 mM Tris and 100 mM NaCl at pH 7.5. To obtain the enzyme from the *E. coli* cells, the cell resuspension was placed under high pressure at 1000 psi in a French Press (SLM-AMICO) and then moved to atmospheric pressure. This caused the cells to rupture and produce a crude cellular extract. A 500  $\mu$ L aliquot of protease inhibitors (Sigma) were added to the *E. coli* cells before rupturing to prevent degradation of the desired protein. The lysed cellular extract was centrifuged at 15,000 rpm (31,000 x g) for 20 min. to separate the desired, soluble supernatant fluid from the insoluble pellet material.

The supernatant liquid was then incubated with 1 mM ATP and 1 mM  $Mg^{2+}$  for 30 min. at 28°C in order to dissociate bound chaperonin proteins. The solution was then passed through a column (13 cm height, 1.8 cm diameter) packed with 3 mL HisPur™ cobalt affinity resin (Thermo), which contains cobalt(II) ion that binds to the 6x histidine tag located on the amino terminal end of the recombinant protein. The column was washed once with 50 mL of lysis buffer to remove non-bound proteins. The column was then resuspended in 10 mL of lysis buffer containing 5 mM ATP, 5 mM  $Mg^{2+}$ , and 20 mM imidazole, and incubated again for 30 min. at 28°C to remove any remaining chaperonin protein. After draining, the column was washed with 50 mL of lysis buffer and 20 mM imidazole to remove any proteins with significant histidine character. The full length and truncated CCT protein was eluted from the column by using 10 mL of lysis buffer containing 200 mM imidazole and collected in 500  $\mu$ L aliquots. The side chain of histidine contains an imidazole ring, therefore the imidazole competes with the

6x histidine tag for binding to the immobilized cobalt. Once the histidine was released from the cobalt, the CCT protein was released from the column.

### **Determination of Protein Concentration by Method of Bradford**

The Bradford assay was employed to determine the concentration of protein in the crude cellular extract, supernatant, and column elution fractions. This method uses a Bio-Rad reagent that binds to the proteins and changes from the cationic form to the neutral form which absorbs light at a wavelength of 595 nm (Bradford, 1976). A standard curve was completed using known concentrations of bovine serum albumin (BSA) that was used to solve for unknown protein concentrations. The Bio-Rad reagent is a 5x solution, meaning it must be diluted fivefold in the prepared sample. When using 1000  $\mu\text{L}$  as the total volume, 200  $\mu\text{L}$  of Bio-Rad reagent was added. The other 800  $\mu\text{L}$  is a mixture of water and protein sample. The unknown samples should have an absorbance somewhere between the most concentrated and least concentrated standard. Once the unknown samples were prepared, the absorbance at 595 nm was determined and this was used to find the mass of protein ( $\mu\text{g}$ ) in the sample according to the standard curve. The concentration ( $\mu\text{g}/\mu\text{L}$ ) could then be found by dividing this mass by the volume of purified protein used in the sample ( $\mu\text{L}$ ).

## **Sodium Dodecyl Sulfate Polyacrylamide Gel Electrophoresis**

Sodium dodecyl sulfate polyacrylamide gel electrophoresis (SDS-PAGE) is a procedure for separating proteins based on molar mass. The polyacrylamide gel consists of a mixture of acrylamide, bis acrylamide, tetramethylethylenediamine (TEMED), buffers, water, and ammonium persulfate. TEMED generates free radicals from ammonium persulfate that promote production of free radical acrylamide monomers which react with non-radical monomers causing polymerization. Acrylamide polymers crosslink with bis acrylamide creating a mesh work of polymers that causes the separation of proteins based on mass. Typically 12% (v/v) acrylamide was used, but the percentage was increased or decreased based on the mass of the protein to be analyzed.

Sample preparation for SDS-PAGE involved diluting protein samples to 1  $\mu\text{g}/\mu\text{L}$  with water to a final volume of 75  $\mu\text{L}$ , adding 25  $\mu\text{L}$  of 4x SDS dye (270 mM SDS, 6 mM bromophenol blue, 200 mM Tris-HCl, 400 mM DTT, 40% (v/v) glycerol) to a final concentration of 1x in 100  $\mu\text{L}$ , and boiling the samples for 5 min. This causes denaturing and allows negatively charged SDS molecules to evenly coat the protein. The samples and a set of standards of known molar mass were loaded onto the gel. The proteins were then separated at 200 V for 50 min. After electrophoresis, the gel was incubated in a 0.1% (w/v) staining solution of coomassie blue dye dissolved in 45% (v/v) methanol and 10% (v/v) acetic acid for 20 min. The gel was destained to remove stain not bound to protein by incubating the gel in a solution of 45% (v/v) methanol and 10% (v/v) acetic acid. Comparing the migration of the standard proteins to the unknown samples allowed for estimation of the molar mass of the proteins in the elution fractions and identification of CCT and CCTrun.

## Western Blot Immunoassay

Western blot immunoassay was used to track the desired protein throughout the affinity column purification fractions. Western blots are performed by first separating a protein mixture on an SDS-PAGE gel followed by protein transfer to a polyvinylidene difluoride (PVDF) membrane. A WesternBreeze® kit (Invitrogen) was used for Western blot development using the following procedure. The membrane was first treated with a blocking solution consisting of milk proteins, saline, and detergent for 30 min. to prevent non-specific binding of the primary antibody. Next, the membrane was subjected to 2 washes, 5 min. each, with ultra-filtered water. The primary mouse anti-His antibody (Invitrogen), diluted 1:20,000 in blocking solution, was then incubated with the membrane for 1 hr. The mouse anti-His antibody binds specifically to the 6x histidine tag found at the amino terminus of the desired protein. The membrane was washed 4 times for 5 min. each with an antibody wash solution from the kit to remove any primary antibody weakly bound to the PVDF membrane. A goat anti-mouse IgG secondary antibody conjugated to alkaline phosphatase was then incubated with the membrane for 30 min. at room temperature. This goat antibody has specificity for the primary mouse antibody, thus increasing sensitivity of the blotting procedure. The membrane was washed 4 times for 5 min. each with the antibody wash solution and 3 times for 5 min. each with ultra-filtered water before the chromogenic substrate was added. The chromogenic substrate contained 5-bromo-4-chloro-3-indolyl-1-phosphate (BCIP), the substrate for alkaline phosphatase, and nitro blue tetrazolium (NBT), which produces color when the BCIP is digested by the enzyme. Purple bands on the membrane corresponded to 6x-His tagged CCT and CCTtrun protein.

### **Determination of Enzyme Activity using Radioisotope Assay**

Enzymatic activity of CCTtrun was determined using a radioisotope scintillation assay previously developed in the lab for a *D. melanogaster* CCT isoform (Helmink and Friesen, 2004). This was performed by incubating CCT trun with the substrates phosphocholine (PoC) and cytidine 5'-triphosphate (CTP) in a solution containing 50 mM Tris and 10 mM MgCl<sub>2</sub> at a pH of 7.5 with a final volume of 100 µl. A small percentage (12.5% v/v) of the PoC is <sup>14</sup>C-labeled, serving as a tracer to monitor conversion of PoC to CDP-choline. Reactions were terminated by addition of 100 µl of 150 mM unlabeled PoC in 10% trichloroacetic acid (TCA). Then, 500 µl of a 10 mg/mL suspension of activated charcoal was incubated with the reaction mixture for 30 min. on ice to bind the product CDP-choline. The charcoal was washed twice with 500 µL of H<sub>2</sub>O by vortexing, pelleting the charcoal at 11,000 rpm (13,500 x g) for 3 min., and decanting the supernatant liquid. Finally, 500 µL of 10% (v/v) acetic acid was added to release the CDP-choline product from the charcoal, followed by vortexing and pelleting the charcoal at 11,000 rpm (13,500 x g) for 3 min. The supernatant liquid containing CDP-choline was added to 5 mL of ScintiSafe 30% scintillation fluid (Fisher Scientific) and placed in a Beckman LS 3000 scintillation counter.

The scintillation counter output is in counts per minute (cpm) which was converted to nmol product formed/min/mg of enzyme, calculated using a formula. First, the background cpm, from an assay tube containing no CCTtrun activity, were subtracted from the experimental counts per minute. Next, the difference was divided by fraction recovery, assay time in min., specific activity of [<sup>14</sup>C]PoC in cpm/nmol, and amount of enzyme in mg. To determine fraction recovery, a tube containing no enzyme but

containing some cpm of [ $^{14}\text{C}$ ]CDP-choline was assayed alongside the rest of the enzyme samples. The scintillation counter revealed the amount of [ $^{14}\text{C}$ ]CDP-choline present after the assay process and these counts were termed the recovered cpm. In the final step, the recovered cpm were divided by the initially added cpm to yield the fraction recovery. The specific activity of [ $^{14}\text{C}$ ]PoC was calculated by counting a volume of [ $^{14}\text{C}$ ]PoC equal to the volume used in the assay. The cpm of [ $^{14}\text{C}$ ]PoC were then divided by the volume of [ $^{14}\text{C}$ ]PoC, in  $\mu\text{L}$ , and the concentration of the [ $^{14}\text{C}$ ]PoC sample, in mM.

This quotient yielded the specific activity of [ $^{14}\text{C}$ ]PoC, which was then changed to cpm/nmol. Finally, the values for the recovery fraction and specific activity of PoC were used to find the specific activity of CCTrun in units of nmol of CDP-choline/min/mg of CCTrun enzyme.



## **Determination of Kinetic Parameters and the Effects of Divalent Metal Cations, Temperature, and pH on Enzyme Activity**

The maximal velocity ( $V_{max}$ ) of an enzyme is the specific activity level at which the enzyme is saturated and the ratio of product formed per amount of enzyme remains the same over time. The substrate constant ( $K_m$ ) is the concentration of substrate at half of the  $V_{max}$ . Both of these kinetic parameters were determined for CCTrun for both CTP and PoC by varying the concentration of one substrate while holding the other constant. A concentration of 1 mM CTP was used when varying PoC concentration and 30 mM PoC was used when varying CTP concentration. All assays contained 5  $\mu$ g of purified CCTrun enzyme, buffer consisting of 50 mM Tris and 10 mM  $MgCl_2$  at a pH of 7.5, and water to a final volume of 100  $\mu$ l incubated at 37°C for 30 min.

The effect of different divalent metal cations on CCTrun activity was assessed using 10 mM of  $MgCl_2$ ,  $CuNO_3$ ,  $FeSO_4$ ,  $CaCl_2$ ,  $ZnCl_2$ ,  $NiCl_2$ ,  $MnCl_2$ , or  $CoCl_2$  in an assay with 5  $\mu$ g of purified CCTrun enzyme, 1 mM CTP, 30 mM PoC, 50 mM Tris buffer at a pH of 7.5, and water to a final volume of 100  $\mu$ l incubated at 37°C for 30 min. The effect of temperature on CCTrun activity was shown using a standard assay with 5  $\mu$ g of purified CCTrun enzyme, 1 mM CTP, 30 mM PoC, 50 mM Tris buffer at a pH of 7.5, and water to a final volume of 100  $\mu$ l incubated for 30 min. at several temperatures. Finally, the effect of pH on CCTrun activity was determined using buffers of varying pH in a standard assay with 5  $\mu$ g of purified CCTrun enzyme, 1 mM CTP, 30 mM PoC, and water to a final volume of 100  $\mu$ l incubated at 37°C for 30 min. All enzyme assays were developed and specific activity determined as previously described.

## Two-Step Cloning of the Amplified RFP and *Leishmania* Genes into a Plasmid Expression Vector

The generation of expression vectors used for localization of fluorescent proteins by confocal microscopy required cloning using a LEXSYcon2 Expression Kit (Jena Bioscience). This kit uses *L. tarentolae*, a non-pathogenic strain of *Leishmania*, for protein expression by transformation using the pLEXSY-sat2 plasmid vector (Figure 11).

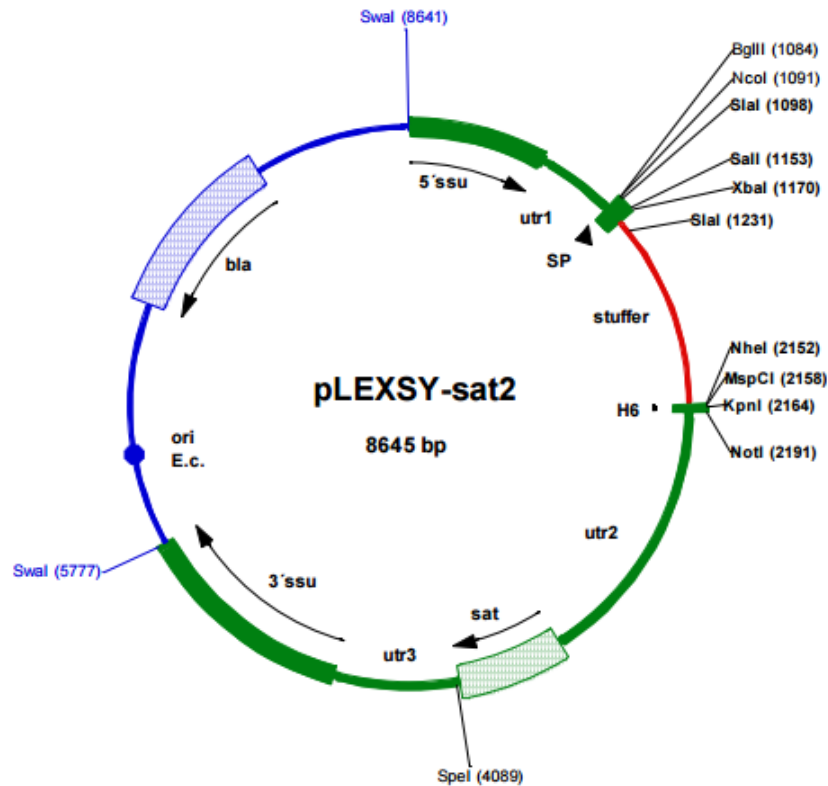


*Figure 11.* Plasmid Map of pLEXSY-sat2. The BglII (1084) and KpnI (2164) restriction sites were used to clone the RFP gene. The plasmid also contains a carboxy-terminal 6x histidine sequence. Genes encoding  $\beta$ -lactamase for selective resistance against penicillin-type antibiotics in bacteria and encoding streptothricine acetyltransferase (SAT) for selective resistance against nourseothricin (NTC) in *Leishmania* are also present. Plasmid also contains a 5'ssu and 3'ssu sites for homologous recombination into the *Leishmania* host chromosome after linearization with Swa I (5777).

The generation of fluorescent protein expression vectors involved two repeating instances of the molecular cloning, transformation, and plasmid purification previously described. To summarize, the mCherry gene was amplified by PCR using the RFP5' forward and RFP3' reverse oligonucleotide primers (Table 2).

Table 2

*Localization Experiment Primer Sequences and Restriction Sites*

| Name    | Oligonucleotide Sequence                                     | Restriction Enzyme |
|---------|--|--------------------|
| RFP5    | 5'-TGCAGATCTCGAGGATATCTAGAGCTA<br>GCGCCATGGTGAGCAAGGGCGAG-3' | BglII<br>XbaI      |
| RFP3    | 5'-TCGAGCAGGTACCCTTGTACAGCTCGTCC<br>ATG-3'                   | KpnI               |
| LmCCT25 | 5'-TCGAGCAGATCTGCCATGCCGCATCTG<br>CTTGAGC-3'                 | BglII              |
| LmCCT23 | 5'-TCGAGCTCTAGATGCCCGTCCTTCACC-3'                            | XbaI               |
| LmECT5  | 5'-TCGAGCAGATCTGCCATGCCACCGTTT<br>CTTCG-3'                   | BglII              |
| LmECT3  | 5'-TCGAGCTCTAGAGCTTGCCTCCCG-3'                               | XbaI               |

*Note.* Forward (5') and reverse (3') oligonucleotide primer sequences are listed. Start codons are noted in green.

The mCherry insert DNA generated using PCR and the pLEXSY-sat2 vector were verified on 0.7% agarose gel. The mCherry insert and pLEXSY-sat2 vector were then digested separately with Bgl II and Kpn I. The mCherry insert DNA was ligated to the pLEXSY-sat2 vector using T4 DNA ligase. The ligation mixture was then be incubated

with competent DH5 $\alpha$  *E. coli* cells, and successful transformation was tested by growth on LB agar plates supplemented with 100 mg/mL of ampicillin at 30°C. This incubation temperature was decreased relative to the normal growth protocol due to minor instability of the pLEXSY-sat2 plasmid. Colonies were then picked from the plates, cultured, and plasmid DNA was isolated. Plasmid samples were screened for successful ligation of the mCherry insert by re-digestion with Bgl II and Kpn I and run on a 0.7% agarose gel. This entire process was then repeated using CCT and ECT insert generated by PCR from *L. major* genomic DNA and the recombinant pLEXSY-sat2-mCherry plasmid vector digested with Bgl II and Xba I. As previously shown, a restriction site for XbaI was made in the forward RFP5' primer and was then inserted with the ligated RFP gene into the pLEXSY-sat2 plasmid to allow for ligation of the *L. major* CCT and ECT genes to the 5' end of the RFP gene (Table 2).

### **Growth and Transformation of *L. tarentolae* Cells**

Non pathogenic *L. tarentolae* were reactivated from glycerol stocks and cultured in 10 mL of brain-heart infusion (BHI) suspension media in a ventilated tissue culture flask at 26°C. Cells were passaged in a 1:10 dilution and continually supplemented with 50 µL of 10 µg/mL penicillin and streptomycin to prevent bacterial contamination, as well as 20 µL of a 0.25% solution of porcine hemin every 3-4 days. Heme, which *Leishmania* obtain from the blood of their host *in vivo*, is necessary for respiration and the growth of these parasites as obligate aerobes. The density, shape, and motility of these cells were monitored by microscopy.

A separate restriction digest was performed to linearize the recombinant pLEXSY-sat2-RFP-CCT and pLEXSY-sat2-RFP-ECT expression vectors by incubating 5 µL of each plasmid, 2 µL of 10x NEB buffer #3, 0.5 µL of *Swa*I, and 12.5 µL of water at 25°C overnight. This linearization of the plasmid using the blunt-end cutting *Swa*I is necessary for integration of the expression cassette into the *L. tarentolae* chromosome by homologous recombination using the 5'ssu and 3'ssu sites. Both the plasmid vectors were run on a 0.7% agarose gel, excised, and purified using the PureLink™ Quick Gel Extraction Kit (Invitrogen).

A healthy and motile 10 mL culture of *L. tarentolae* cells, diluted the previous day, was grown to a density of approximately  $6 \times 10^7$  cells/mL. The cells were then centrifuged at 2,000 x g for 5 min., resuspended in half the volume of the supernatant, and put on ice for 10 min. A 350 µL aliquot of cells was then added to 5 µg of pLEXSY-sat2-RFP-CCT and pLEXSY-sat2-RFP-ECT linearized DNA in separate electroporation cuvettes. The cells were electroporated at 450 V, 450 µF, and a 5 msec pulse time using

a GenePulser Xcell™ electroporator (Bio-Rad). Following electroporation, the cells were incubated in freshly supplemented BHI media overnight. The next day, 10 µL of 100 mg/mL NTC was added to the electroporated culture in order to select for *Leishmania* cells that had successfully transformed and integrated the desired gene, as well as the SAT cassette, into their chromosome. Successive passage and dilution ensured the growth of healthy, dense recombinant strains of *L. tarentolae* expressing CCT-mCherry and ECT-mCherry fusion proteins.

### **Fixing and Staining of Cells for use in Confocal Microscopy**

A 10 mL culture sample of recombinant *L. tarentolae* expressing CCT-mCherry and ECT-mCherry fusion proteins were harvested 3 days after 1:10 dilution and centrifuged at 2,000 x g for 5 min. The mCherry fluorophore absorbs green light ( $\lambda_{\max} = 587$  nm) and emits red light ( $\lambda_{\max} = 610$  nm). The cells were then washed by resuspending in 500  $\mu$ L of phosphate buffered saline (PBS) and centrifuged. Cells were fixed by resuspending in 200  $\mu$ L of 2% (v:v) paraformaldehyde in PBS for 20 min. and centrifuged. The fixative was then washed off by resuspending in 1 mL of PBS and centrifuged. The cells were permeabilized by resuspending in 500  $\mu$ L of 0.2% (v:v) Triton X-100 in PBS (PBT) for 20 min. and centrifuged. A 200  $\mu$ L amount of labeling solution containing SYBR green (also courtesy of Dr. Kevin Edwards) was then added to the cells. The labeling solution consisted of 2  $\mu$ L of SYBR green in 1 mL of PBT and was kept in the dark due to sensitivity to fluorescence bleaching. SYBR green absorbs blue light ( $\lambda_{\max} = 497$  nm) and emits green light ( $\lambda_{\max} = 520$  nm) and is used to stain DNA, which is present in both the nucleus and kinetoplast of *L. tarentolae*.

Slides were prepared for confocal microscopy by adding 5  $\mu$ L of labeled cells to mounting media and placing between a slide and coverslip. Recombinant cells were visualized using the TCS SP2 Confocal Microscope (Leica), utilizing a HCX PL APO 63X oil immersion objective, a blue Ar 488 nm laser to see SYBR green, and a green DPSS 561 nm laser to see mCherry. Lastly, images were overlaid to visualize sub cellular localization of both CCT and ECT within the *L. tarentolae* cell.

## CHAPTER III

### RESULTS AND DISCUSSION

#### **Putative LmCCT and LmECT Amino Acid Sequence Alignment and Analysis**

The genome sequences of *Leishmania major* are available through the Sanger Institute (<http://www.sanger.ac.uk>) and were analyzed for genes involved in PC biosynthesis. A putative CCT gene was identified and its encoded amino acid sequence was aligned with isoforms from *P. falciparum*, *C. elegans*, and the rat using the Clustal Omega alignment tool (<http://www.ebi.ac.uk/Tools/msa/clustalo/>) and BoxShade server ([http://www.ch.embnet.org/software/BOX\\_form.html](http://www.ch.embnet.org/software/BOX_form.html)) (Figure 12).



```

LmCCT      1  MPHLLEHSFLFTTEERQLIYHANS DVNTRPVGVFVTRIFYP IWICI SKHLLSDLVAPNAIT
LmCCT      61  LAGLLSSMQAYQLINTYYHFGNQQHD PHAVLVVDVKS SLQAFGLRGAGQVPLAAEKTUVGE
LmCCT     121  MASAYKAGPGAAAKTAKAMGAAAAAATAA SAASGQILRPPETDYVDF FHTDRTVQTAT
LmCCT     181  VLAILLLVTSITCGSLDGVHARRCRSAT SLGDI FSRICSSMARVFMALITLLEVFQIEDVC
LmCCT     241  TKWYFLALQLIELNTVLGRI SASNLKKDRVKNLAYIATYCFRESEL SFLMVLLLIARWF
PfcCCT      1  -----MDSSN
LmCCT     301  YPTACRDLGLVILAKAQVGYNTLVVATFVS IALLKMKKLYKGI ILLCLAAARVLPFLYLLP
PfcCCT      6  YFHDCTMLSEH-----
CelCCT      1  -----FIHK-----
RatCCTa     1  -----MDAQS-----
LmCCT     361  LSQYSLLSVIGDAMMVGLLSIEVYVSHLAQRRIHAAVFLCLGSLL----N-----VLSV
PfcCCT     18  --NESSESSNNDI--NGKQKE-----HI--KKGNS-ENQDVDPDTNPDVAFDDDDDDMS
CelCCT      6  --QEKLPQRKRTMDSPEEDV-----EVKHKATE-VEYVVRSLASDEPAFPSEALAITT
RatCCTa     6  --SAKNSKAKKEVPGPNGA-----TE-EDGIP-SKVQRCAVGLRQPAPFSEIEVDFS
LmCCT     413  AGSIMELIAMLVLDLSYSINVPLFTFVRNVELDGVEDLCHAGHKKLMALK--FGNRLIV
PfcCCT      67  NDESESESSQMDSEPNKGS IKNSK-NVVTYADGVLDMLHGHMKQDEAKKLFENTYLLIV
CelCCT      58  REAVDPSKKIT--LMAEAENEAGR-PVRIYADGIYDLPFHGHANQRVVKKMFPNVYLLIV
RatCCTa     57  K--PWVRVIM--EEACRGTFCER-PVRVYADGIYDLPFHGHARALMCAKMLFPNTYLLIV
LmCCT     471  GVCSDEECASLRPPMTTDERINELRLCKYVSEMI PNSSVVTGDTAEMRYYNHVVWCG
PfcCCT     126  GVTSQNETKLRGQVQTLBERTETKHIRVDEMI SPQPFVVV-TEEPKRYKDYVAHD
CelCCT     115  GVCGDRDTHNRGRITITSEPERYDGRHCRVYDEMYREDFWFC-TVEPKNLKDFVAHD
RatCCTa     111  GVCSDELTHNRGFTIMNEPERYDAVQHCYVDEIVRNAPNTL-TEEPKAEHRDFVAHD
LmCCT     531  E-----EYNTPTDLYAVPFRMGILCTVETPGISTSVLISRRA
PfcCCT     185  DIPYANNQKKKKKSKGKSFDFDEENEDIFAWLFRAGKFKATQRTGVTSTDLIVRILK
CelCCT     174  AIPYVAP-----GEEDEYKELREGMFLTEPTEGISTSDIVCRHIR
RatCCTa     170  DIPYSSA-----GSDVVKHDEAGMFAPTQRTGISTSDIVRIVR
LmCCT     571  ASISSIEAKDRSDKPTVKDGA-----
PfcCCT     245  NYEDYIERSLQGIHPNELNIGVTKAQS IKMKKNI LRWGEKVTDELTKVTLTKPLGTFD
CelCCT     216  DYDKYVRRNLQGGYSPKELNVGFLAASKYQIQNKVDSLK-----
RatCCTa     212  DYDVIYARRNLQGGYTAKELNVSFINEKKYHLQERVDKVKKVKDV-----EEKSKEF
PfcCCT     305  DQGVENRQVKFKEPFKIWKMA SNKLI TDFTKLEATSYLTSIQ----NIIDYEIEMDDYA
CelCCT     255  -----S---KGIELLSTWKSDDIIRDFIDTFHKDGGLNAGGGRLLKGMMSRSPSPSP
RatCCTa     264  VQKVEE---KSIDLIQKWEKRSREFIGS FLEMPGPEGALKHMLKEGKGRMLQAI SPKQSP
PfcCCT     361  SSNFDEETS-----
CelCCT     307  H----EGSPTGI-EHHLETQD-EEEEEALEEKVVVEQKIVEKKEVVKKRS SRNFAKTP
RatCCTa     321  SSSPTHERSPSPSFRWPFSGKTS PSSSPASLSRCKAVTCDISEDEED-----

```

Figure 12. Amino Acid Sequence Alignment of CCT Isoforms. *L. major* CCT (accession XP\_001682542.1), *P. falciparum* CCT (accession AAK11280.1), *C. elegans* CCT (accession P49583.2), and Rat CCT (accession NP\_511177) are aligned using Clustal Omega and BoxShade programs. Amino acids highlighted in grey represent those that are similar, and those highlighted in black are identical. A possible transmembrane domain is highlighted in green. A nuclear localization signal is highlighted in blue. The truncated portion of the protein containing the cytidylyltransferase catalytic domain is highlighted in yellow.

The *L. major* CCT cDNA is 1779 bp long coding for 592 amino acids. The putative CCT sequence from *L. major* contains amino acids shown to be critical for catalysis by the rat isoform. There are several conserved cytidyltransferase sequences, including the 451-HxGH and 555-RTxGxST motifs and K481 shown to be critical for catalysis in rat CCT $\alpha$  (Lee et al., 2009). The presence of the highly conserved catalytic region suggested that the putative CCT of *L. major* would be able to catalyze the conversion of phosphocholine and CTP to CDP-choline. However, an interesting observation is that the *L. major* isoform appears to lack the lipid binding and phosphorylation regions present in other CCT isoforms, suggesting it may not be regulated by membrane association or reversible phosphorylation. Less noticeably, it lacks a nuclear localization signal, which indicated it does not localize to the nucleus in *Leishmania*, but does contain an extensive amino-terminal sequence of about 350 amino acids not seen in other CCT isoforms. This region was shown to have significant hydrophobic character and possibly contain a transmembrane region upon analysis by hydropathy plot using the Kyte-Doolittle hydrophobicity index (<http://web.expasy.org/protscale/>) (Figure 13).

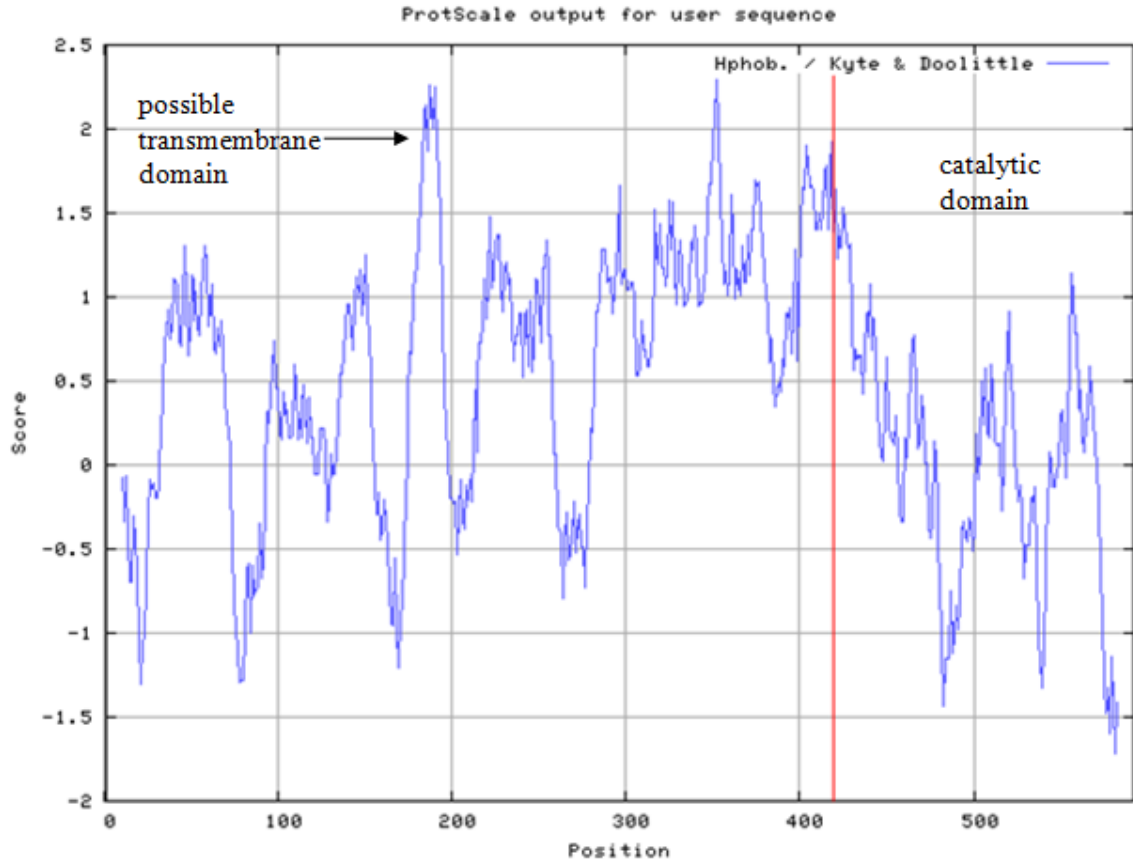


*Figure 13.* Hydropathy Plot of *L. major* CCT. Kyte-Doolittle hydrophobicity index was used to construct plot, wherein more hydrophobic amino acids have more positive scores and more hydrophilic amino acids have more negative scores. A window size of 19 amino acids was also used to indicate possible transmembrane regions with a peak above 1.8. The vertical red line indicates position of CCT truncation mutagenesis at position 422.

The truncation mutation beginning at the 422 position was designed in order to clone the carboxy terminal catalytic region by itself, under the suspicion that this unique amino terminal region may have limited solubility and low protein expression due to its hydrophobic nature. The presence of a possible transmembrane domain in this region also indicated that CCT might permanently localize to membranes in the *Leishmania* cell such as the endoplasmic reticulum.

Sequence alignment of the ECT gene from *L. major* also showed conservation of the signature cytidylyltransferase motifs, indicating the ability to catalyze the conversion of CTP and phosphoethanolamine to CDP: ethanolamine (Figure 14).

```

CrECT 1 MVLDSVKQNFLLW CAAGVVLGVSLLSWKAAKAAELVYPIQYQYRPGTISGWLANALA
ratECT 1 -----MIRNGHGAG-----GA
LmECT 1 MPTVSSSTPS-----PASTPTVGVVPGKVVWLNADPNDEYSLFC
TbECT 1 -----MKRSVSVKVVWLNEDTPNDPYPLVA

CrECT 61 NHSKSRKRREVRVVDGCFIMMHFGHANELROAFAMGDDELIVGLINDAEIMRCKGPPVM
ratECT 12 AGLKGGGGQRTVRFVVDGCFIMVHGHSHNQLROAFAMGDDELIVGVHTDDEIARFKGPPVF
LmECT 40 TEAIPKVPVGTVRVVDGCFIMHFGHANELRRARFGDDELIVGCHSDDEVMRFGKPPIM
TbECT 24 PSPLPKRPGTIRVVDGCFIMHFGHANELROAFAMGDDELIVGCHTDDEIIRFKGPPBM

CrECT 121 NEEERHTLDEVRVVDDELITGVVFDLNPFEVMELEFTRHRIDRIHGGDDPCDLPDGSDAFA
ratECT 72 TQEERKMQQIRVVDVWPAAVYVTTLE----TLDKHNDFCVHGMNITITVIGRDTFE
LmECT 100 HAEERYEADRACVVDHVVENYVYCTRLLK----DIERFEIDVHGGDDISVDLNGRNSYQ
TbECT 84 RQEERYEARACKVVDVAVIEGYVYVTRVE----DMKDFEVDVHGGDDISVDLNGRNSYQ

CrECT 181 HAKKLSRFRVVRTEGVSTTDLVGRMLTCSRNVHFINADEPHPLAKSFSMGTPREESN--
ratECT 128 EVKQAGRYECCRTQVSTTDLVGRMLLVTKAHHSSQEMSSSEYREYADSFQKPPHPTPAG
LmECT 156 EIIDAGKFRVVRTEKGISTTDLVGRMLLCTKNHMLKSVDEV-----
TbECT 140 AIIDAGMEFAVVRTECVSTTDLVGRMLLCVPSSELLSDADKK-----

CrECT 239 -----AEASTSDASTRTTLSKFTTTSRRLVQFVSNGRVAPEGARIVVYDGAFTCFHPGH
ratECT 188 DTLSSSEVSSQCPGGQSPWTVGVSQFVDTSQKLIQFASGKEPQFGETVIVYDGAFTLPHIGH
LmECT 197 -QLENSLLE-----HSPTMPCVITTSRRLVQFVSNNSSEKPGDRIVYDGSFDLPHIGH
TbECT 181 -LLDSEV-A-----RKRGPHTTTSRRLVQFVSNKLAPPVATVVYDGAFTLPHASH

CrECT 292 VKILQAAKAQ--GDFLLVGGHTDELVQARAGPHLPIMNLHERSLSVLSCRYVDVVVIGSP
ratECT 248 VDFLQEVVHKLAKRPVVIAGLHFDQVQVNRVYVGENYVIMNLHERLSVLAQRYVSDVVIGAP
LmECT 248 IRVFLQKAREL--GDFVIAGVYEDQVWNEHNGENYVIMSFMERVLGVLSCRYVDVVVIGAP
TbECT 231 IRVFLQKAREL--GDFLLVGGHDDQVRESVGEHFPIMSLNERALGVLSCRYVDVVVIGAP

CrECT 350 CVITEDLMTTFNISVVRGSMSETSMLGPVEEERVEVPRFMGLTETDPSVSDVARNIYH
ratECT 308 YSVTAEILLNHFKDDLVCHG-KDQIVP-DRDGSDFVEPPRRGIFCQIDSGSDLTITLIVQ
LmECT 306 FDVSKQVWIDGLHINVVVGDKFSDLVV-EEGGSTRVEVPRFMGIHEVDGGCILSTDSLID
TbECT 289 RGVVQEMIKILDKVACGTSSETRN-CKGAFDVVEVPRSLNLEKVVVESSDLSSTIMIVE

CrECT 410 RIVDKGAAAFEMRYAKRVVGGVEAYYTGAQVVOEL-----
ratECT 366 RIIKNSLEYEARVQKREAKGLAFLAALRQQAQPRGETD-----
LmECT 365 RIVVENLDFLRCAERRIKDKTSQ-----EIKPDEYRKLREAS
TbECT 348 RIVVKNVLLRQFLRHMQSEAE-----LRKPDVYRNVREV-

```

Figure 14. Amino Acid Sequence Alignment of ECT Isoforms. *C. reinhardtii* ECT (accession AAP21826.1), rat ECT (accession NP\_446020.1), *L. major* ECT (accession XP\_001685405.1), and *T. brucei* ECT (accession XP\_829470.1) are aligned using Clustal Omega and BoxShade programs. Amino acids highlighted in grey represent those that are similar, and those highlighted in black are identical. A possible transmembrane domain involved in localization to the mitochondria is highlighted in red.

The sequence of the *L. major* isoform, however, did not contain the approximately 50 amino acids found in the amino terminus of the isoform from the green algae *C. reinhardtii*. This region forms a possible transmembrane domain that causes

localization to the mitochondria in *C. reinhardtii*, therefore its absence indicated that *L. major* ECT was likely cytosolic (Yang et al., 2004). This is the case in the vast majority of ECT isoforms. The absence of a possible transmembrane domain, as well as any significant hydrophobic character, was also confirmed by hydropathy plot analysis (Figure 15).

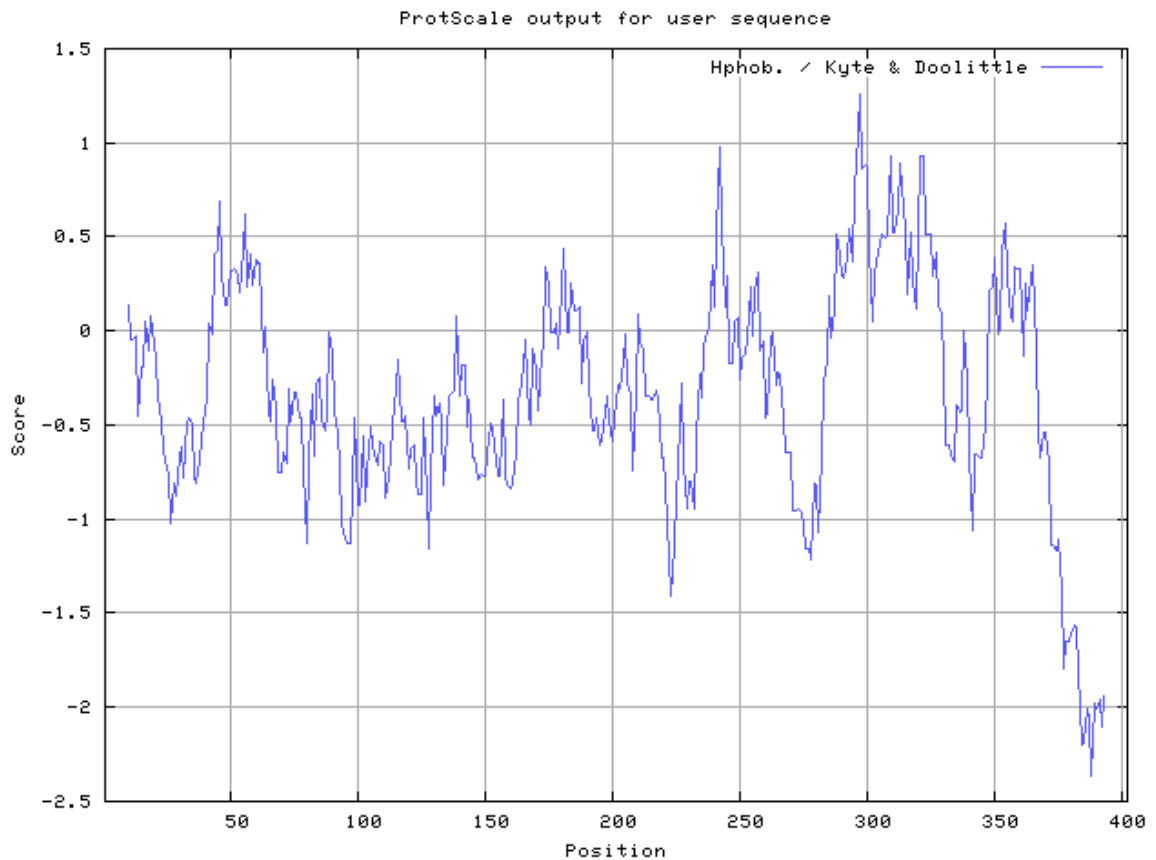


*Figure 15.* Hydropathy Plot of *L. major* ECT. Kyte-Doolittle hydrophobicity index was used to construct plot, wherein more hydrophobic amino acids have more positive scores and more hydrophilic amino acids have more negative scores. A window size of 19 amino acids was also used to indicate possible transmembrane regions with a peak above 1.8.

## Molecular Cloning of the Full Length and Truncated LmCCT Genes into pET45b

Using PCR and the specific oligonucleotide primers, DNA fragments of approximately 1792 bp and 526 bp, for the full length and truncated CCT gene respectively, were amplified from *L. major* genomic DNA. The estimated band size on the agarose gel for each insert included the actual gene sizes plus the 5' and 3' flanking regions added by the oligonucleotide primers. In the case of both reactions, the addition of 2  $\mu\text{L}$  of 50 mM  $\text{MgSO}_4$  allowed for the greatest amplification of DNA (Figure 16).

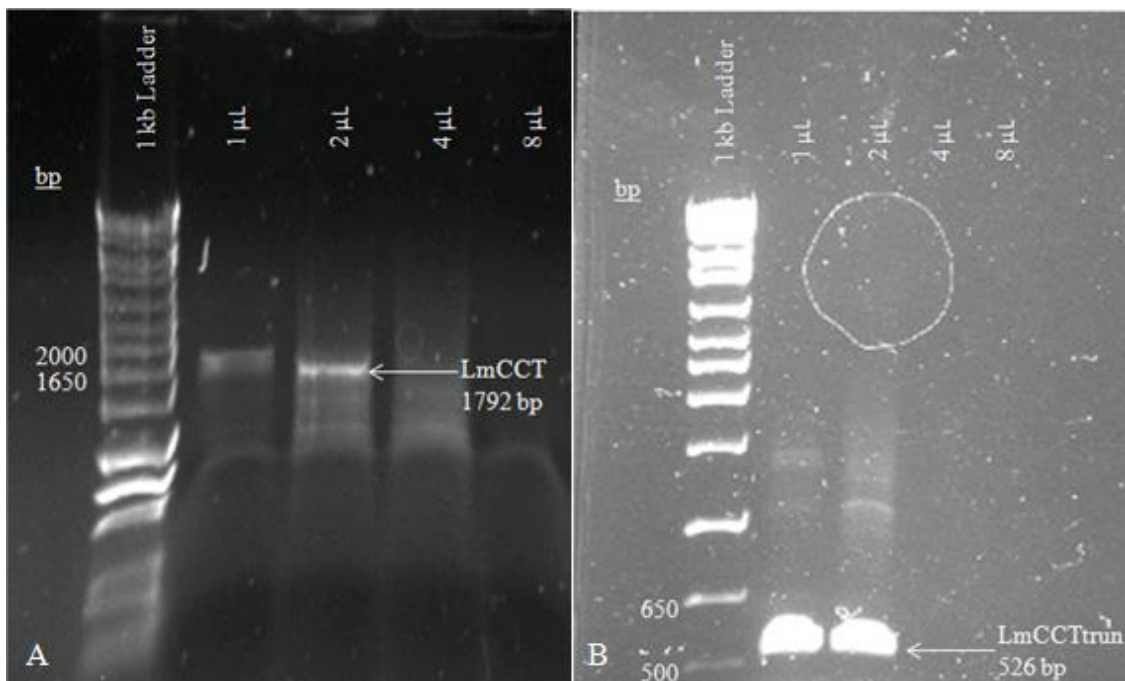


*Figure 16.* Agarose Gels of Amplified LmCCT and LmCCTtrun PCR Products. PCR was conducted using 1, 2, 4, and 8  $\mu\text{L}$  of 50 mM  $\text{MgSO}_4$ . 1 kb DNA ladder was used as the standard. (A) The band observed at approximately 1792 bp corresponds to the amplified LmCCT gene. (B) The band observed at approximately 526 bp corresponds to the amplified LmCCTtrun gene.

Restriction endonuclease digestion with BamHI and XhoI of both the LmCCT and LmCCTtrun PCR products yielded 1776 bp and 510 bp DNA fragment inserts respectively. Digestion of the 5260 bp pET45b plasmid removed a 61 bp “stuffer region” in the multiple cloning site to give a 5199 bp vector (Figure 17).

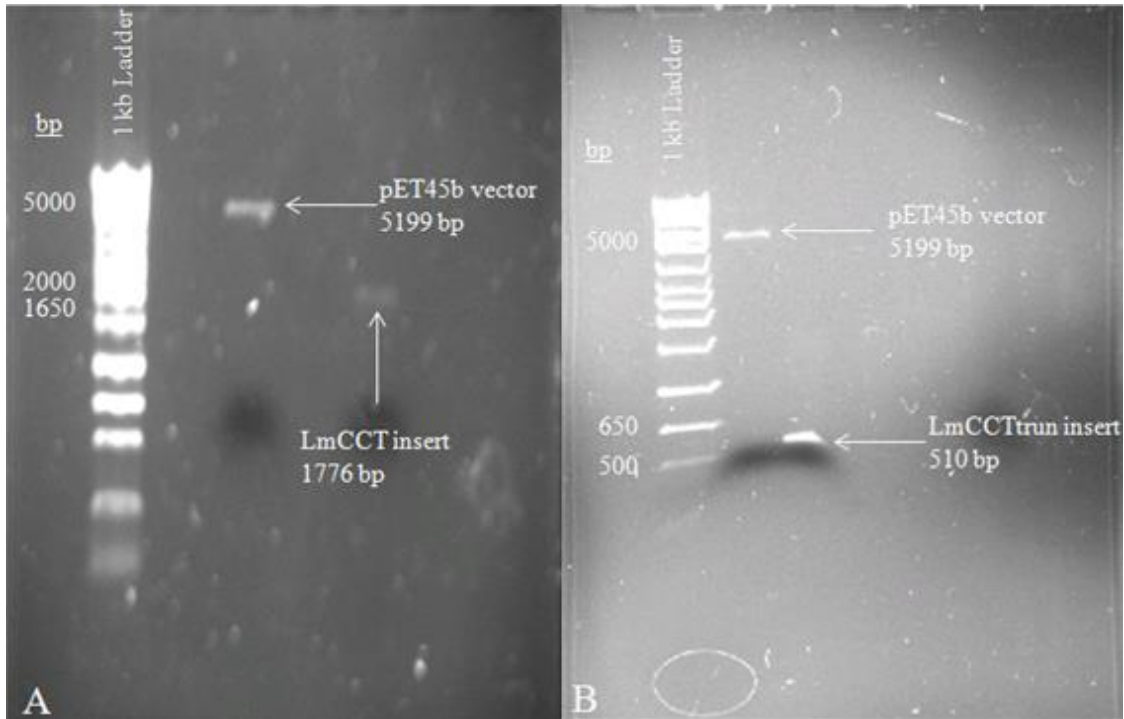


*Figure 17: Agarose Gels of Digestion of LmCCT and LmCCTtrun PCR Products, as well as pET45b, with BamHI and XhoI. 1 kb DNA ladder was used as the standard. The band observed at approximately 5199 bp corresponds to the digested pET45b plasmid vector. (A) The band observed at approximately 1776 bp corresponds to the digested LmCCT insert. (B) The band observed at approximately 510 bp corresponds to the digested LmCCTtrun insert.*

This facilitated ligation and formation of the recombinant plasmids pET45b-LmCCT and pET45b-LmCCTtrun. To verify that the recombinant DNA contained the correct insert, plasmid DNA was purified in high concentration from 18 transformant



colonies grown on selection plates containing LB and ampicillin. Each recombinant plasmid preparation was then subjected to another digestion with BamHI and XhoI to show removal of the desired insert, if present. Digestion of recombinant plasmid DNA purified from several colonies showed successful ligation of the correctly sized gene inserts. Incomplete digestion of the 6975 bp pET45b-LmCCT plasmid and 5709 bp pET45b-LmCCTtrun plasmid was also observed in some of these colonies. Digestion of the original pET45b plasmid vector, or that which had religated with the stuffer region, may have occurred in colonies that failed to produce the desired insert fragment (Figure 18).

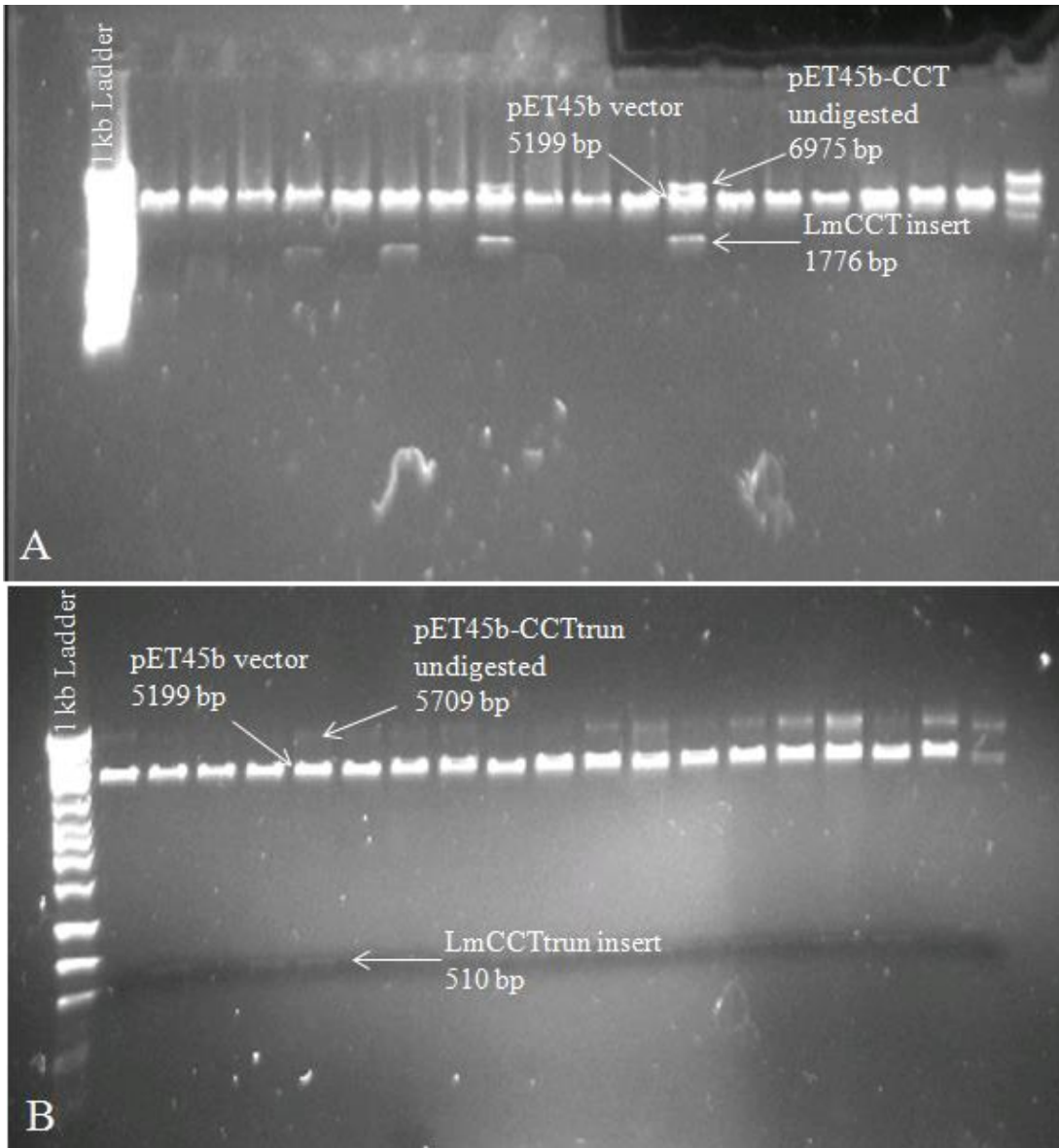


*Figure 18.* Agarose Gel of pET45b-LmCCT and pET45b-LmCCTtrun Redigest with BamHI and XhoI. 1 kb DNA ladder was used as the standard. The band observed at approximately 5199 bp corresponds to the digested original pET45b plasmid vector. (A) The band observed at approximately 1776 bp corresponds to the digested LmCCT insert, which indicates successful ligation and formation of the pET45b-LmCCT recombinant plasmid. The band observed at approximately 6975 bp corresponds to undigested recombinant plasmid. (B) The band observed at approximately 510 bp corresponds to the digested LmCCTtrun insert, which indicates successful ligation and formation of the pET45b-LmCCTtrun recombinant plasmid. The band observed at approximately 5709 bp corresponds to undigested recombinant plasmid.

DNA sequencing verified the identity of the LmCCT and LmCCTtrun gene inserts and showed no discrepancy according to the published sequence.

### **Purification of Truncated CCT**

After confirming the successful cloning of the pET45b-LmCCT and pET45b-LmCCTtrun recombinant plasmids, these expression vectors were used to transform Arctic Express (DE3) RIL cells. This particular strain of *E. coli* is optimized for protein expression using Cpn10 and Cpn60, chaperonin proteins that hydrolyze ATP to ADP to form a heptameric ring structure, which facilitates proper protein folding at low temperatures. After sufficient growth, the cells were ruptured and the protein was purified using immobilized metal affinity chromatography. Unfortunately, the full length CCT enzyme was not able to be expressed in the cells as shown by analysis of purification fractions by SDS-PAGE and Western blot (Figure 19).

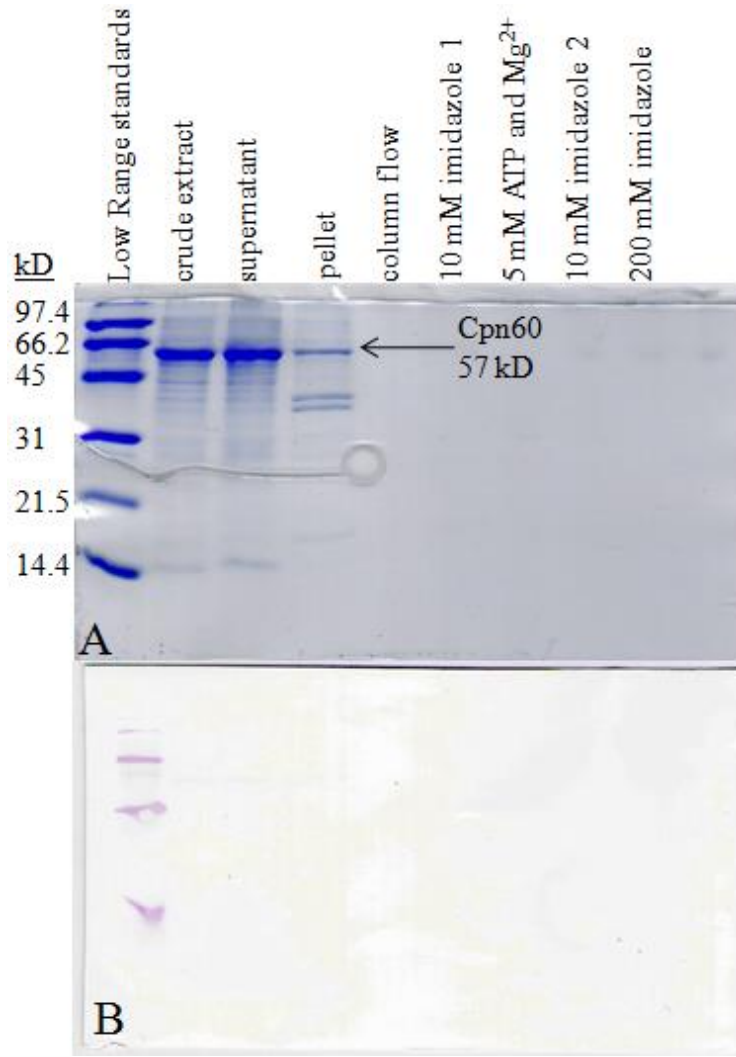


*Figure 19.* Analysis of Full Length CCT Purification Fractions by SDS-PAGE and Western Blot. (A) SDS-PAGE analysis of consecutive purification fractions shows a lack of a band at approximately 67 kD, which would correspond to the full length CCT protein. The band at 57 kD corresponds to Cpn60 chaperonin protein. (B) Western blot analysis shows lack of detection of His-tag labeled protein, confirming the inability of the full length CCT enzyme to be produced.

However, the truncated CCT enzyme was able to be expressed, most likely due to an increased ability to properly fold because of the absence of the highly hydrophobic amino terminal region. Initially, analysis by SDS-PAGE showed a large amount of Cpn60 eluting with the CCTtrun in the 200 mM imidazole fraction, suggesting that the two were still associated. Previous studies of enzyme assays using recombinant Cpn10/60 from *O. antarctica* showed that nearly 100% of Cpn10/60 protein resumed its non-folding, double-ringed, tetradecameric, quaternary structure upon incubation with 2 mM ATP for 30 min. at higher temperatures of at least 28°C (Ferrer et al., 2004). Thus, the novel purification method for separating Cpn10/60 and CCTtrun was created by adding ATP (and coordinating  $Mg^{2+}$ ) to displace the ADP, which would induce the formation of the non-folding tetradecameric structure at high temperatures, and release the bound CCTtrun. This was done in the supernatant solution in order to increase binding of CCTtrun by eliminating steric hindrance of the binding of the 6x His-tag of the protein and the  $Co^{2+}$  in the affinity column resin. The column was also subsequently washed with ATP in order to remove any chaperonin proteins that were still bound. Elution with 200 mM imidazole yielded pure CCTtrun enzyme and its identity was confirmed by Western blot (Figure 20).

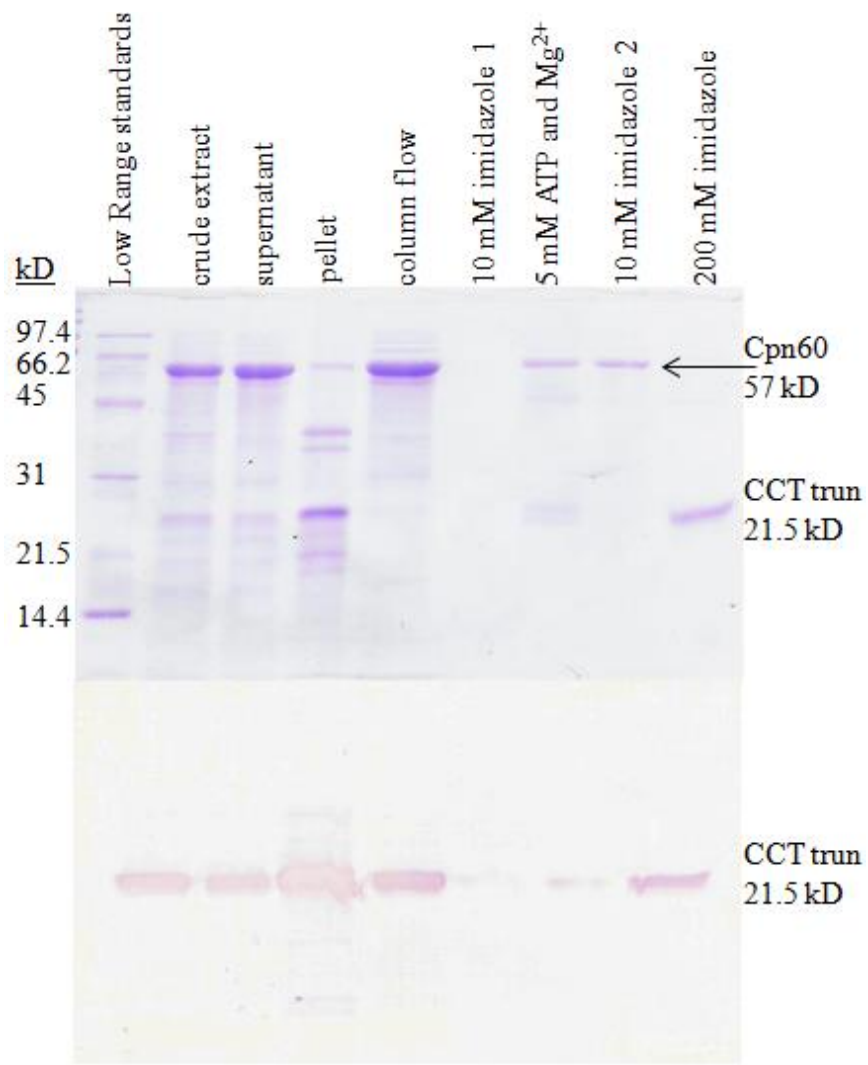


*Figure 20.* Analysis of Truncated CCT Purification Fractions by SDS-PAGE and Western Blot. (A) SDS-PAGE analysis of consecutive purification fractions shows a band at approximately 21.5 kD, corresponding to the truncated CCT protein. The soluble protein is unexpectedly seen in the pellet fraction, which may be due to a low concentration of misfolded protein. The band at 57 kD corresponds to Cpn60 chaperonin protein. Its presence in the column flow through, 5 mM ATP wash, and second 10 mM imidazole wash, as well as its absence in the 200 mM imidazole elution indicates the success of the novel Cpn10/60 purification method. (B) Western blot analysis shows detection of His-tag labeled protein, confirming the presence of the truncated CCT enzyme in the 200 mM imidazole elution fraction.

As a result, the column retained about 15% of total protein of the cell extract from the cellular supernatant, and the combined washes managed to remove about 6% of total protein. The most highly concentrated 500  $\mu$ L elution fraction contained 0.236 mg of purified CCTrun, accounting for 0.226% of total protein in the cell extract (Table 3).

Table 3

*Purification of CCTrun by Metal Affinity Chromatography*

| Fraction                             | Sample Volume (mL) | Protein Concentration (mg/mL) | Total Protein (mg) | % Yield |
|--------------------------------------|--------------------|-------------------------------|--------------------|---------|
| Crude Extract                        | 20                 | 5.21                          | 104                | (100)   |
| Supernatant                          | 20                 | 4.83                          | 96.5               | 92.7    |
| Pellet                               | 20                 | 0.221                         | 4.43               | 4.25    |
| Flow Through                         | 50                 | 1.62                          | 80.9               | 77.7    |
| 10 mM Imidazole 1                    | 50                 | 0.004                         | 0.191              | 0.183   |
| + 5 mM ATP and 5 mM Mg <sup>2+</sup> | 10                 | 0.072                         | 0.717              | 0.689   |
| 10mM Imidazole 2                     | 50                 | 0.104                         | 5.20               | 5.00    |
| 200mM Imidazole                      | 0.5                | 0.471                         | 0.236              | 0.226   |

*Note.* Purified CCTrun was eluted from the Co<sup>2+</sup> affinity column using 10 mL of 200 mM imidazole and collected in 20 aliquots of 500  $\mu$ L. The sixth aliquot contained 0.236 mg of CCTrun enzyme, representing 0.226% of total cellular protein.



## Characterization of the Kinetic Properties of Truncated CCT

The catalytic activity of purified *L. major* CCT<sub>trun</sub> was dependent on the concentration of substrates phosphocholine (PoC) and cytidine 5'-triphosphate (CTP) according to Michaelis-Menten kinetics. Increasing concentrations of each substrate showed a corresponding increase in specific activity following a curve that reached an asymptote at the apparent  $V_{max}$  where the enzyme activity was saturated. A curve was fit to the data using the Hill equation.

The Hill equation,  $V_o = \frac{v_{max}[S]^n}{K_m + [S]^n}$ , is a slight derivation of the Michaelis-Menten equation wherein each term in the equation raised to the power of the "Hill coefficient" (n). Thus, while showing enzyme saturation as a function of substrate concentration, the presence of the coefficient in the Hill Equation allows for determination of the level of cooperativity in the binding of each substrate. Cooperativity refers to the effect that binding one molecule of substrate by the enzyme has on its affinity for other substrate molecules. This may indicate the presence of multiple, and possibly allosteric, binding sites on the same polypeptide, and/or the presence of a multimeric protein with subunits containing homologous binding sites. A Hill coefficient value greater than 1 indicates positive cooperativity, a value less than 1 indicates negative cooperativity, and a value equal to 1 indicates no cooperativity. SigmaPlot® nonlinear regression analysis was used to determine the parameters of the curve fitted to the data using the Hill equation. Thus, the  $V_{max}$  and  $K_m$  for CTP were found to be approximately 351 nmol/min/mg and 0.0648 mM respectively, while the Hill coefficient was 2.04

(Figure 21 A). Also, the  $V_{max}$  and  $K_m$  for PoC were found to be approximately 396 nmol/min/mg and 3.74 mM respectively, while the Hill coefficient was 0.953 (Figure 21 B).

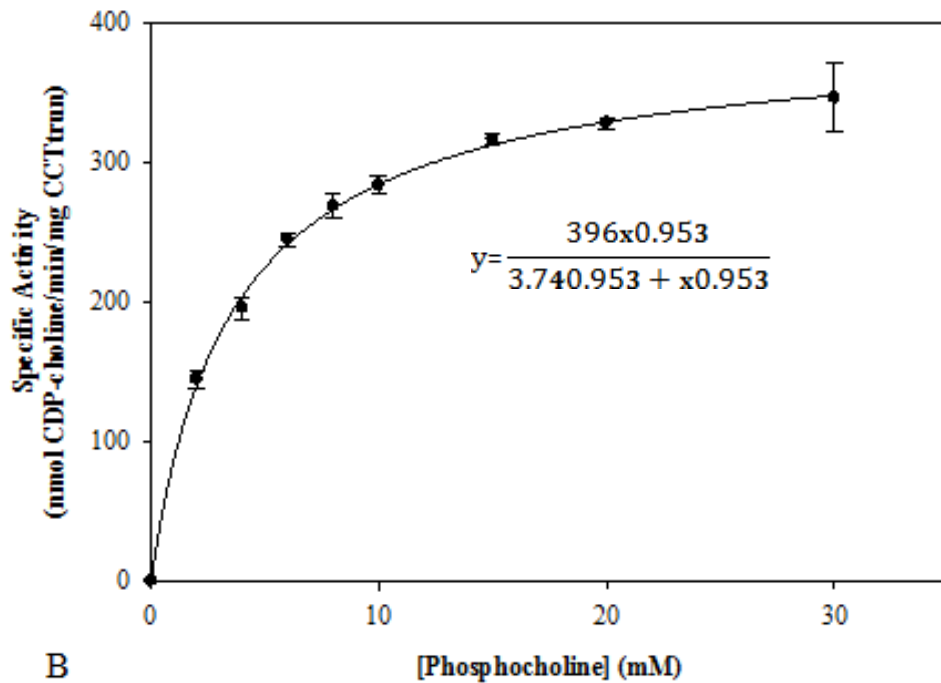
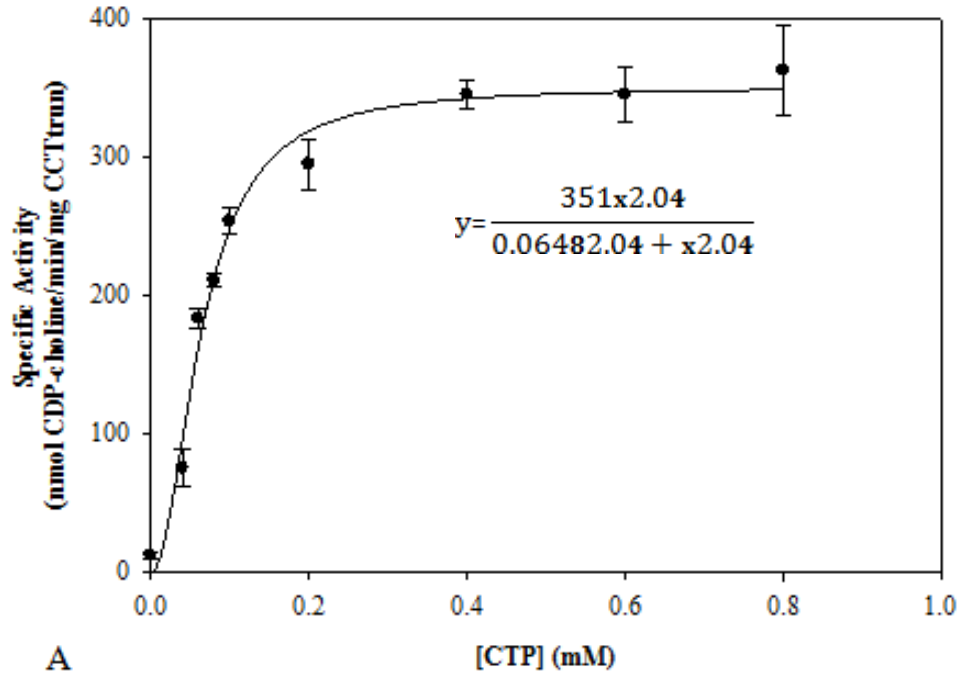


*Figure 21.* Substrate Dependence Curves of CTP and Phosphocholine. Each data point is the average of triplicate measurements and the standard error is indicated by the error bars. Hill Equation was used to fit curve to data and nonlinear regression analysis software was used to determine kinetic parameters. (A) Specific activity as a function of CTP concentration. (B) Specific activity as a function of PoC concentration.

Data were also linearized using the double-reciprocal Lineweaver-Burk plot. In this plot, the y-intercept is equivalent to the inverse of  $V_{max}$  and the x-intercept represents the negative inverse of  $K_m$ . Using this representation, the  $V_{max}$  and  $K_m$  for CTP were found to be approximately 625 nmol/min/mg and 0.25 mM respectively (Figure 22 A). Also, the  $V_{max}$  and  $K_m$  for PoC were found to be approximately 400 nmol/min/mg and 3.72 mM respectively (Figure 22 B).

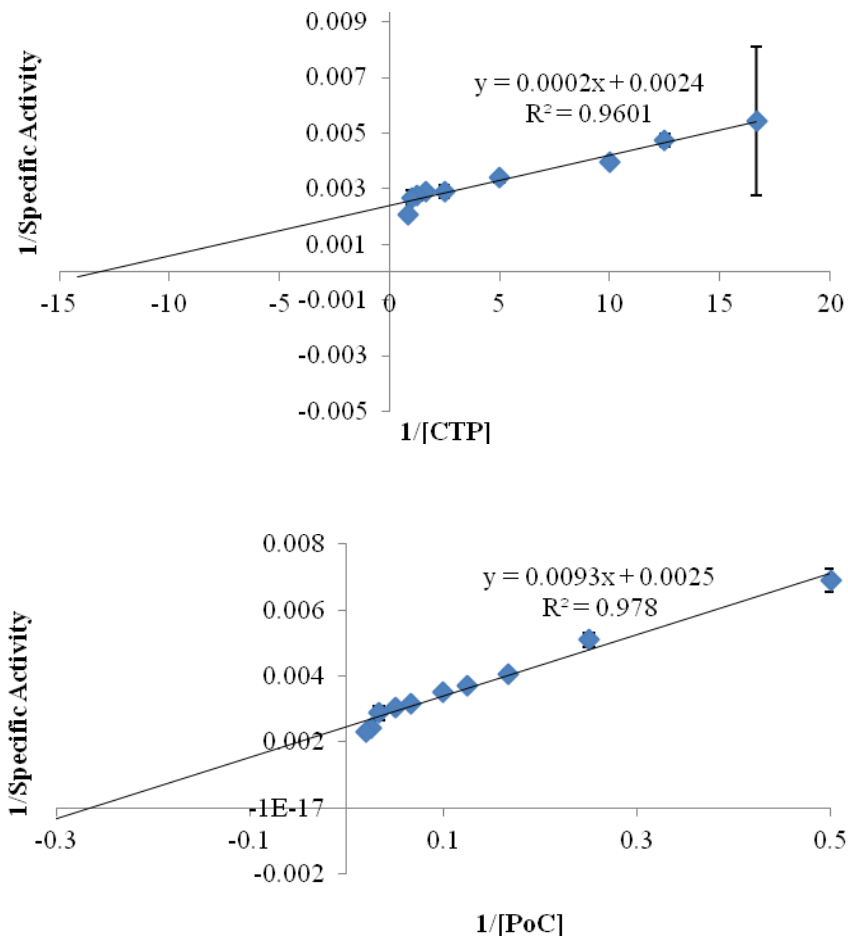


*Figure 22.* Lineweaver-Burk Plots for CTP and Phosphocholine. Each data point is the average of triplicate measurements and the standard error is indicated by the error bars. Apparent  $V_{max}$  and  $K_m$  were calculated using trendline equation. (A) The inverse of specific activity as a function of the inverse of CTP concentration. (B) The inverse of specific activity as a function of the inverse of PoC concentration.

The kinetic parameters determined by the Hill equation nonlinear regression analysis were used in comparison to other CCT isoforms, with  $V_{max}$  being an average of the two values. However, this value was shown to be two to three orders of magnitude lower compared to those reported for full length CCT isoforms from other organisms with the exception of *P. falciparum* at 550 nmol/min/mg. This may indicate a similar

cellular role for the enzyme, and the Kennedy pathway as a whole, in the intracellular parasitic lifestyle shared by these two organisms pertaining to the *de novo* synthesis of phospholipids. The  $K_m$  value utilizing CTP was less than all other isoforms but on the same order of magnitude as that of Dros2. The  $K_m$  value utilizing PoC was greater than all other isoforms but on the same order of magnitude as that of Dros1 (Table 4). These seemingly extreme values for  $K_m$  of both substrates of the enzyme from *L. major* may be explained by a difference of substrate concentration and availability within the macrophage host cell. These kinetic parameters may also be very different than those of the full length enzyme due to the presence of the hydrophobic amino terminal domain, which may allow for regulation of activity by association with membranes.

Table 4

| CCT isoform                    | $V_{max}$ (nmol/mg/min) | $K_m$ (mM) |      |
|--------------------------------|-------------------------|------------|------|
|                                |                         | CTP        | PoC  |
| <i>L. major</i>                | 374                     | 0.0648     | 3.74 |
| <i>Rat <math>\alpha</math></i> | 25480                   | 1.29       | 0.65 |
| <i>D. melanogaster 1</i>       | 23904                   | 1.21       | 2.29 |
| <i>D. melanogaster 2</i>       | 2254                    | 0.81       | 0.63 |
| <i>S. cerevisiae</i>           | 35550                   | 1.42       | 0.80 |
| <i>C. elegans</i>              | 30166                   | 5.2        | 1.6  |
| <i>P. falciparum</i>           | 550                     | 10.9       | 0.49 |

*Kinetic Values of Various CCT Isoforms*

*Note.*  $V_{max}$  and  $K_m$  values for *L. major* CCT<sub>trun</sub> compared to those of other isoforms from the rat (Friesen et al., 1999), *D. melanogaster 1* (Tilley et al., 2008), *D. melanogaster 2* (Helmink and Friesen, 2004), *S. cerevisiae* (Friesen, Park, and Kent, 2001), *C. elegans* (Friesen, Liu, and Kent, 2001), and *P. falciparum* (Yeo et al., 1997).

### **Effect of Various Divalent Metal Cations on Truncated CCT Activity**

Cytidylyltransferases from various model organisms have been reported to use the divalent magnesium cation ( $\text{Mg}^{2+}$ ) as a cofactor to stabilize the negatively charged phosphate groups of CTP during catalysis (Kent, 1997). Nonetheless, catalytic activity of *L. major* CCT was assessed in the presence of a variety of cations, as its available metabolites and cofactors are unique compared to these other organisms due to its parasitic lifecycle. The most interesting result by far was shown by the addition of  $\text{Fe}^{2+}$ , which increased the activity of CCT trun nearly five-fold compared to  $\text{Mg}^{2+}$ . Several cations afforded the CCT trun enzyme a similar level of activity; the highest being  $\text{Mn}^{2+}$  at 87%, next  $\text{Co}^{2+}$  at 84%, and  $\text{Ni}^{2+}$  at 83% compared to  $\text{Mg}^{2+}$ . Other divalent cations were either not utilized efficiently for, or possibly inhibited, catalysis; with  $\text{Zn}^{2+}$  at 5% and  $\text{Ca}^{2+}$  and  $\text{Cu}^{2+}$  showing no activity compared to  $\text{Mg}^{2+}$ . This was very similar to the negative control which contained no divalent cation and showed no activity (Figure 23).



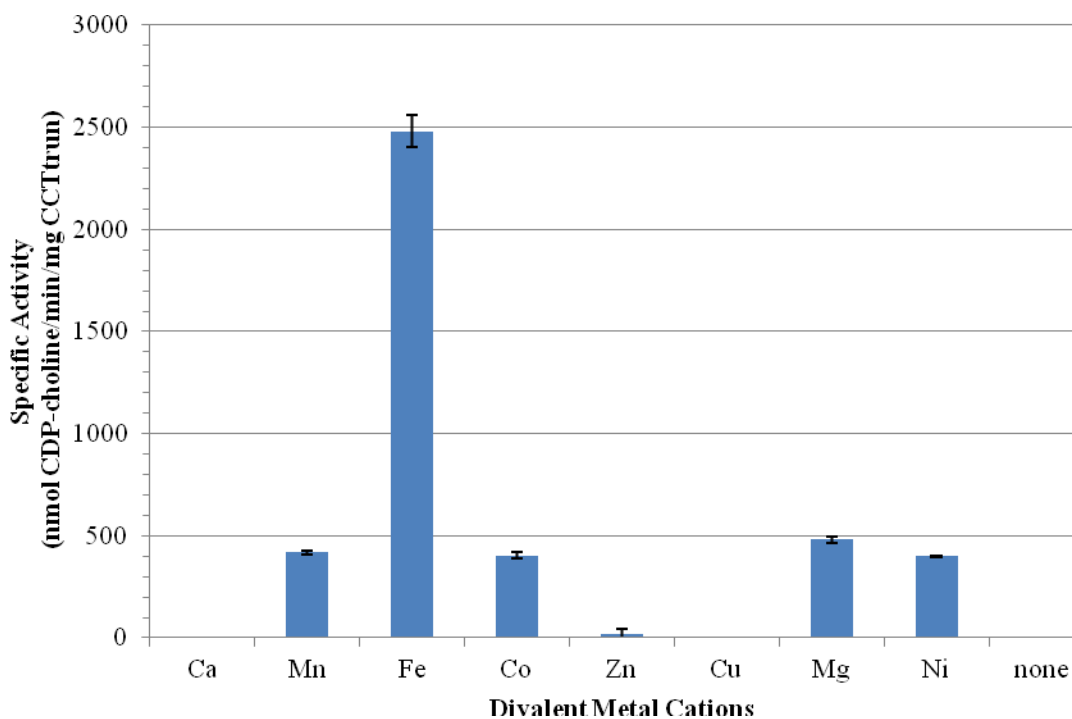


*Figure 23.* Specific Activity of CCTtrun in the Presence of Various Divalent Cations. Each cation has a charge of 2+ and was present at a concentration of 10 mM. Data are the average of three determinations and the standard error is indicated by the error bars.

As yet, no studies exist that show  $\text{Fe}^{2+}$ , or any iron ion, to be used in the cytidyltransferase reaction. Additionally, when a measurement of background was taken of a  $\text{Fe}^{2+}$  reaction with no enzyme, the number of counts accounted for more than 50% of the total. This was considered unacceptably high for the radioisotope scintillation assay, especially when compared to the other divalent cations, and drastically reduced the credibility of this result. However, *L. major* has been shown to express LIT1, a divalent cation membrane transporter which has a preference for  $\text{Fe}^{2+}$  and is transcriptionally up-regulated by iron deprivation. LIT1 is also required for intracellular replication of amastigotes in macrophages and is required for the development of cutaneous leishmanial

lesions in mice (Huynh et al., 2006). Therefore, it is possible that  $\text{Fe}^{2+}$  might cause dramatic activation of CCT, which is the rate controlling enzyme responsible for the *de novo* synthesis of PC, to meet the demand for new phospholipid membrane in the rapidly multiplying cells. This hypothesis is further supported by the lack of expression and activity of PEMT, the other enzyme responsible for PC synthesis, in *Leishmania* amastigotes (Bibis et al., 2014). Concerning the other divalent cations, a previous member of our lab had shown a similar trend in activity with CCT1, a nuclear isoform from *D. melanogaster*, using the same enzyme assay protocol. Activity of CCT1 was actually shown to increase with  $\text{Mn}^{2+}$ , was 85% with  $\text{Co}^{2+}$ , 48% with  $\text{Ni}^{2+}$ , 28% with  $\text{Ca}^{2+}$ , and 25% with  $\text{Zn}^{2+}$  at 5 mM concentrations in reference to  $\text{Mg}^{2+}$  (Tilley et al., 2008).

Ionic radius size may also have a role in the effect of each cation on enzyme activity. The ionic radius of 114 pm, 88 pm, and 87 pm, for  $\text{Ca}^{2+}$ ,  $\text{Zn}^{2+}$ , and  $\text{Cu}^{2+}$  respectively, suggests that these cations may inhibit activity because they are too large to effectively incorporate into the cytidyltransferase active site. This contrasts with  $\text{Fe}^{2+}$ ,  $\text{Mg}^{2+}$ ,  $\text{Mn}^{2+}$ ,  $\text{Co}^{2+}$ , and  $\text{Ni}^{2+}$ , which have ionic radii of 75 pm, 86 pm, 81 pm, 79 pm, and 83 pm (Miessler and Tarr, 2004). Excluding  $\text{Fe}^{2+}$ , these smaller cations may be bound at the enzyme active site but still induce an unfavorable conformation or be unable to efficiently stabilize the phosphate groups present in the substrates, resulting in less activity compared to  $\text{Mg}^{2+}$ .

### **Effect of pH and Temperature on Truncated CCT Activity**

The pH and temperature at which *L. major* CCT attained maximal activity was source of uncertainty due to the difference in growth conditions between its promastigotes and amastigotes forms and how this might impact its intracellular environment. This difference is ultimately due to the difference in host organism; the promastigote being present in the primary sand fly vector and the amastigote in the secondary mammalian host. Specifically, promastigotes are cultured at pH 7.5 and 22-26°C, which imitates the environment of the sand fly midgut (Zilberstein and Shapira, 1994). Amastigotes are grown at pH 5.5 and 37°C, which resembles the microenvironment of the phagolysosome into which the *Leishmania* cell is engulfed by the mammalian macrophage (Vannier-Santos et al., 2002). *L. major* CCT trun activity was higher over the more basic range, with its maximum at pH 7.5 (Figure 24).

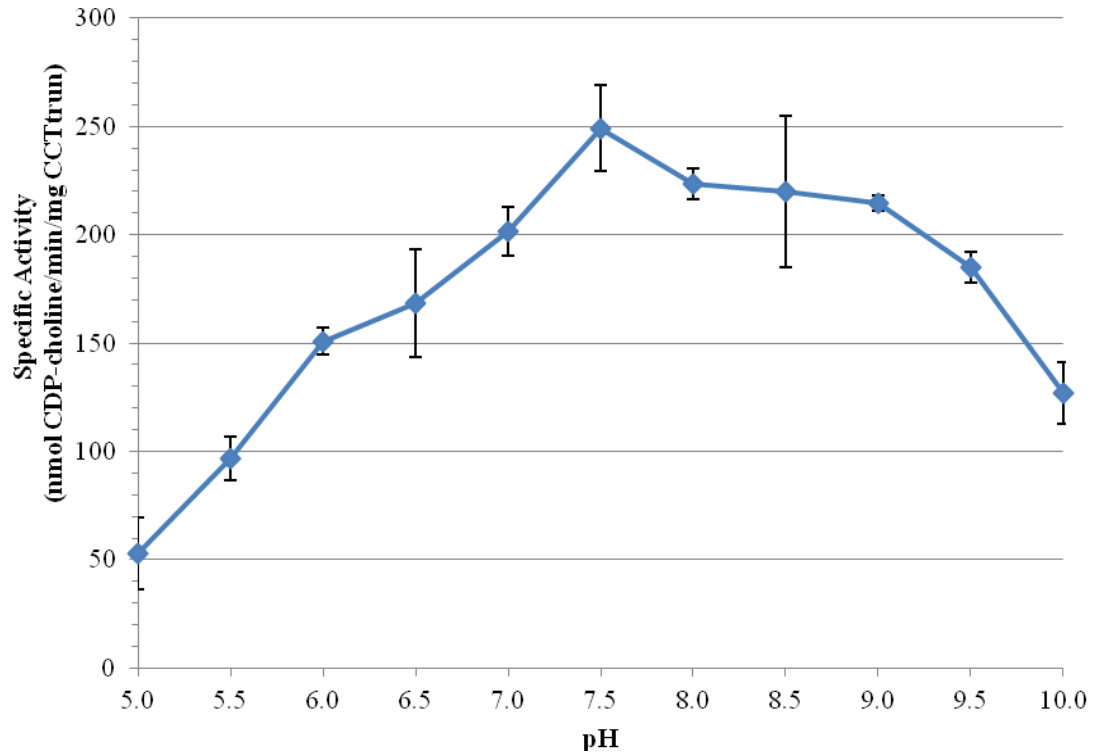


Figure 24. Specific Activity of CCTrun over a Range of pH. Data are the average of three determinations and the standard error is indicated by the error bars.

This indicates that if CCT is active in cell-invasive *L. major* amastigotes, these cells must be able to effectively modulate their intracellular pH in order to withstand the acidic environment of the macrophage phagolysosome. Indeed, this harsh microenvironment is overcome in *L. donovani* amastigotes by the action of a plasma membrane H<sup>+</sup>-translocating ATPase which maintains a neutral intracellular cytoplasmic pH (Glaser et al., 1992). CCT run activity was also highest at 37°C, with only 23% maximal activity at 25°C (Figure 25).

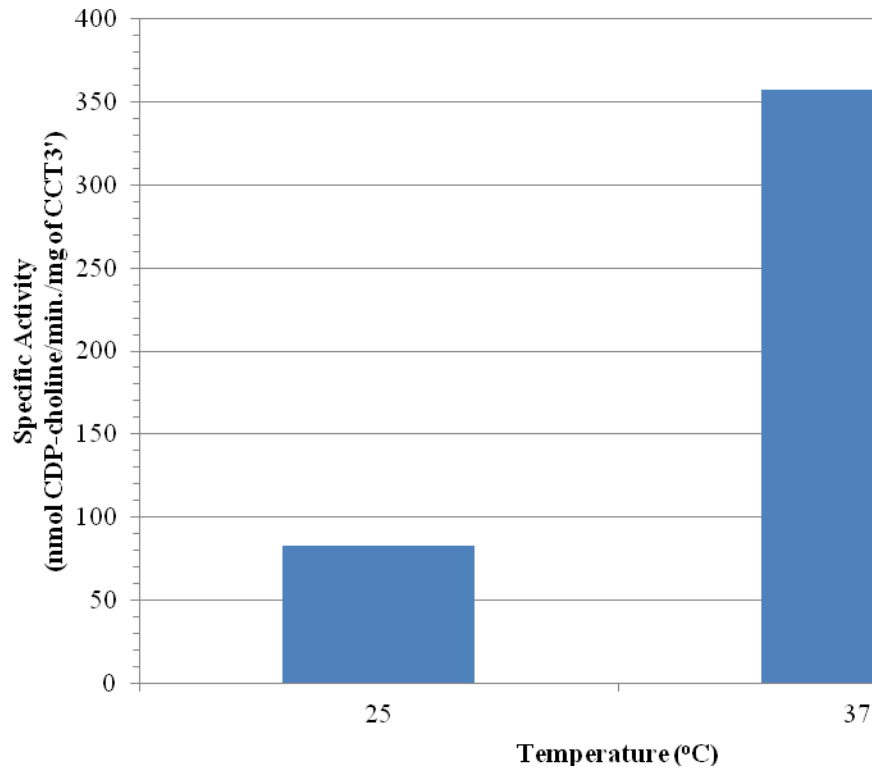
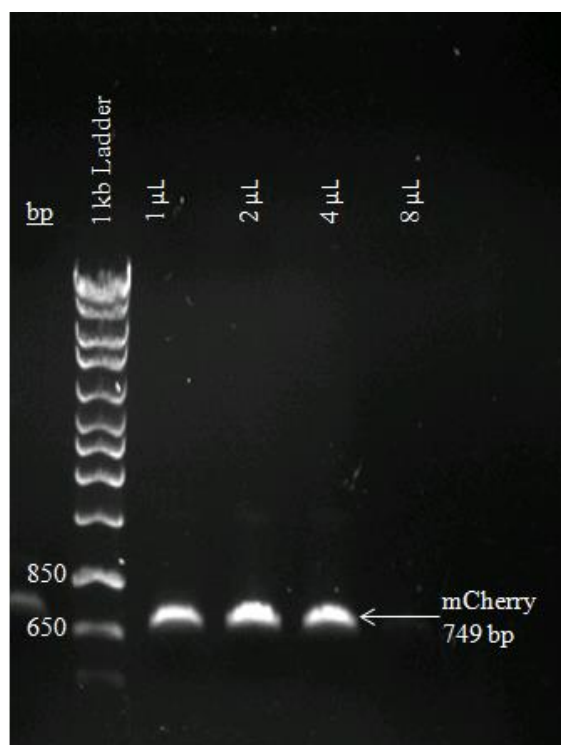


Figure 25. Specific Activity of CCTtrun at 25 and 37°C. Data are the average of three determinations and the standard error is indicated by the error bars.

One may discern from these data that, if expressed, CCT would have the highest activity in *Leishmania* amastigotes compared to promastigotes. Both of these results also correspond well to the enzyme assay conditions of pH 7-7.5 and 37°C that are used for human, rat, *D. melanogaster*, *C. elegans*, and *P. falciparum* isoforms, which may indicate that these conditions are necessary for maximal activity of the conserved catalytic motif across species.

## Two-Step Cloning of the RFP Gene, followed by LmCCT and LmECT Genes, into pLEXSY-sat2

Using PCR and the specific oligonucleotide primers, a DNA fragment of approximately 749 bp for the mCherry gene was amplified from the Hto-RFP plasmid. The estimated band size on the agarose gel for each insert included the actual gene sizes plus the 5' and 3' flanking regions added by the oligonucleotide primers. The addition of 2  $\mu$ L of 50 mM MgSO<sub>4</sub> allowed for the greatest amplification of DNA (Figure 26).



*Figure 26.* Agarose Gels of Amplified mCherry PCR Product. The band observed at approximately 749 bp corresponds to the amplified LmCCT gene. PCR was conducted using 1, 2, 4, and 8  $\mu$ L of 50 mM MgSO<sub>4</sub>. 1 kb DNA ladder was used as the standard.

Restriction endonuclease digestion with BglII and KpnI of the mCherry PCR product yielded a 734 bp DNA fragment insert. Digestion of the 8645 bp pLEXSY-sat2 plasmid removed a 1080 bp “stuffer region” in the multiple cloning site to give a 7565 bp vector (Figure 27).



*Figure 27.* Agarose Gels of Digestion of mCherry PCR Product and pLEXSY-sat2 with BglII and KpnI. The band observed at approximately 734 bp corresponds to the digested mCherry insert. The band observed at approximately 7565 bp corresponds to the digested pLEXSY-sat2 plasmid vector. 1 kb DNA ladder was used as the standard.

This facilitated ligation and formation of the 8299 bp recombinant pLEXSY-sat2-RFP plasmid. To verify that the recombinant DNA contained the correct insert, plasmid DNA was purified in high concentration from nine transformant colonies grown on selection plates containing LB and ampicillin. Each recombinant plasmid preparation

was then subjected to another digestion with BglIII and KpnI to show removal of the desired insert, if present. Digestion of recombinant plasmid DNA purified from several colonies showed successful ligation of the correctly sized gene inserts. Digestion of the original plasmid vector, or that which had religated with the stuffer region, may have occurred in colonies that failed to produce the desired insert fragment (Figure 28).

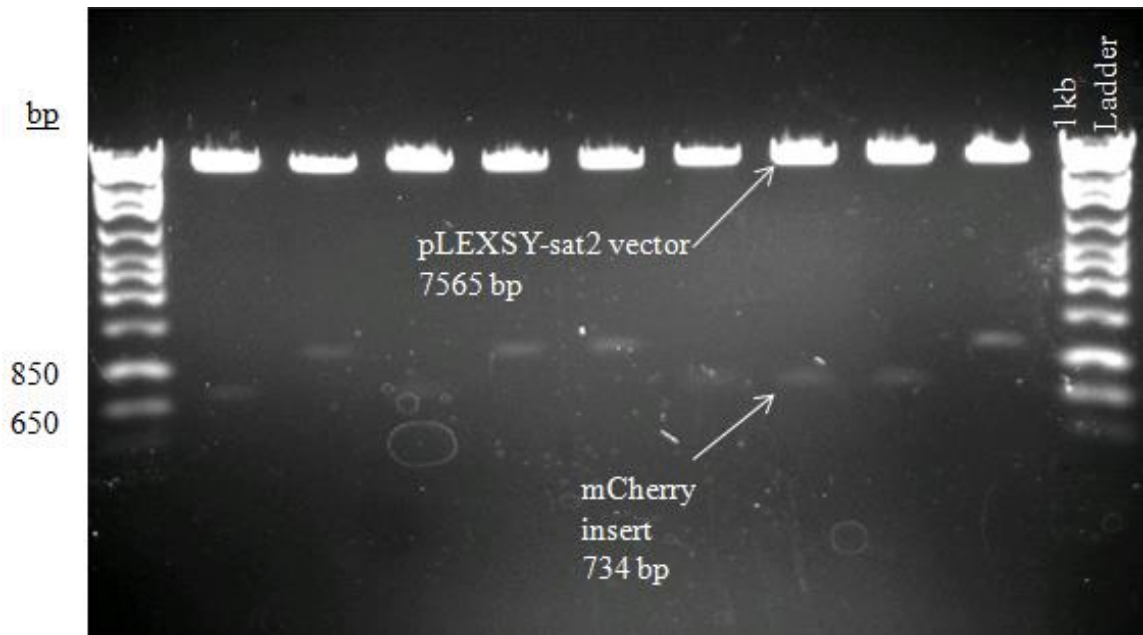


*Figure 28.* Agarose Gel of pLEXSY-sat2-RFP Redigest with BglIII and KpnI. The band observed at approximately 734 bp corresponds to the digested mCherry insert and the band observed at approximately 7565 bp corresponds to the digested pLEXSY-sat2 vector, which indicates successful ligation and formation of the pLEXSY-sat2-RFP recombinant plasmid. 1 kb DNA ladder was used as the standard.

Following the formation of the recombinant pLEXSY-sat2-RFP plasmid vector, both CCT and ECT genes were amplified from *L. major* genomic DNA using a specific set of oligonucleotide primers. The estimated band size on the agarose gel for each DNA fragment insert was 1796 bp and 1236 bp respectively, and included the actual gene sizes



plus the 5' and 3' flanking regions added by the oligonucleotide primers. In the case of both reactions, the addition of 2, 4, and 8  $\mu\text{L}$  of 50 mM  $\text{MgSO}_4$  allowed for the greatest amplification of DNA (Figure 29).

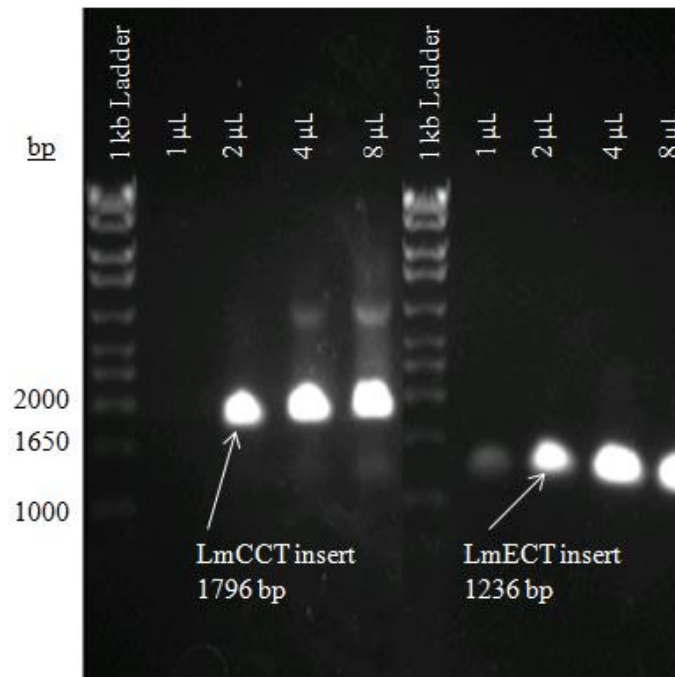


*Figure 29.* Agarose Gels of Amplified LmCCT and LmECT PCR Product. The band observed at approximately 1796 bp corresponds to the amplified LmCCT gene. The band observed at approximately 1236 bp corresponds to the amplified LmECT gene. PCR was conducted using 1, 2, 4, and 8  $\mu\text{L}$  of 50 mM  $\text{MgSO}_4$ . 1 kb DNA ladder was used as the standard.

Restriction endonuclease digestion of the LmCCT and LmECT PCR products with *Bgl*III and *Xba*I yielded 1778 bp and 1218 bp DNA fragment inserts respectively. Digestion of the 8299 bp pLEXSY-sat2-RFP plasmid removed the 14 bp fragment between the two restriction sites that had been designed in RFP5 forward primer, yielding an 8285 bp vector. This facilitated ligation and formation of the recombinant pLEXSY-

sat2-RFP-CCT and pLEXSY-sat2-RFP-ECT plasmids. Digestion of recombinant plasmid DNA purified from ten colonies transformed with the pLEXSY-sat2-RFP-CCT plasmid and one colony with the pLEXSY-sat2-RFP-ECT plasmid by BglII and XbaI showed successful ligation of the correctly sized gene inserts (Figure 30).



*Figure 30.* Agarose Gel of pLEXSY-sat2-RFP-CCT and pLEXSY-sat2-RFP-ECT Redigest with BglII and XbaI. The band observed at approximately 1778 bp corresponds to the digested LmCCT insert (left) and the band observed at approximately 1218 bp corresponds to the digested LmECT insert (right). The band at approximately 8285 bp corresponds to the pLEXSY-sat2-RFP vector. The presence of the insert bands indicates successful ligation and formation of both the pLEXSY-sat2-RFP-CCT and pLEXSY-sat2-RFP-ECT recombinant plasmids. 1 kb DNA ladder was used as the standard.

DNA sequencing verified the identity of the mCherry, as well as the *L. major* CCT and ECT gene inserts, and showed no notable discrepancies according to the published sequences.

### Cellular Localization of *Leishmania Major* CCT and ECT

The LmCCT-mCherry and LmECT-mCherry fusion proteins were both expressed in non-pathogenic *L. tarentolae* to illustrate localization in the native cellular environment any other species specific localization mechanisms. However, it is not known if the location of chromosomal integration of the fusion protein genes using the 5'ssu and 3'ssu homologous recombination sequences in the pLEXSY-sat2 vector caused a difference in localization that was regulated by a specific epigenetic effect. Overlay of the images of the mCherry only control showed mixed fluorescence of the green and red channels in nucleus but not the kinetoplast, as well as ubiquitous cytoplasmic localization throughout the rest of the cell (Figure 31).

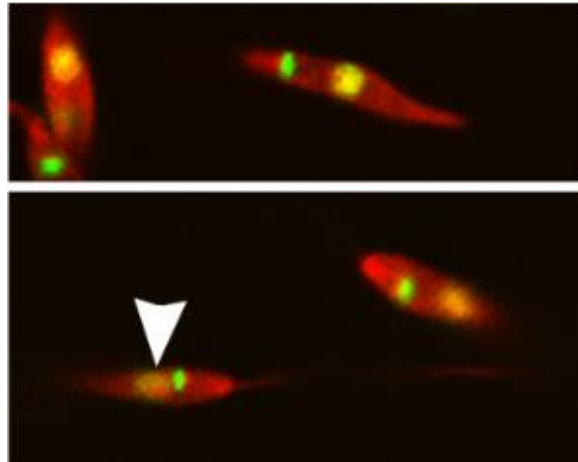


*Figure 31.* Visualization of the mCherry Control by Confocal Microscopy. Overlay of *L. tarentolae* cells visualized in the green and red channels. The larger nucleus and smaller kinetoplast were labeled green by excitation of SYBR green using the blue Ar 488 nm laser. The control was labeled red by excitation of the mCherry tag with the green DPSS 561 nm laser.

Overlay of the CCT images showed no mixed fluorescence of the green and red channels, suggesting that, unlike those found in humans, rat, or *D. melanogaster*, the *L. major* CCT isoform did not localize to the nucleus (Wang et al., 1995; Tilley et al., 2008). The fusion protein localized to the cytoplasm, but showed an irregular and uneven distribution. Thus, it was determined that *L. major* CCT is mostly cytoplasmic, which is further evidenced by nearly all enzyme activity for CCT being found in the supernatant of lysed *Leishmania* cells. CCT may also be able to reversibly associate to internal membranes within the *Leishmania* cell such as the endoplasmic reticulum or plasma membrane, as this occurs with isoforms of CCT from most other organisms as previously described (Kent, 1997). This may explain why it is not so ubiquitously expressed in the cytoplasm as the mCherry only control (Figure 32).

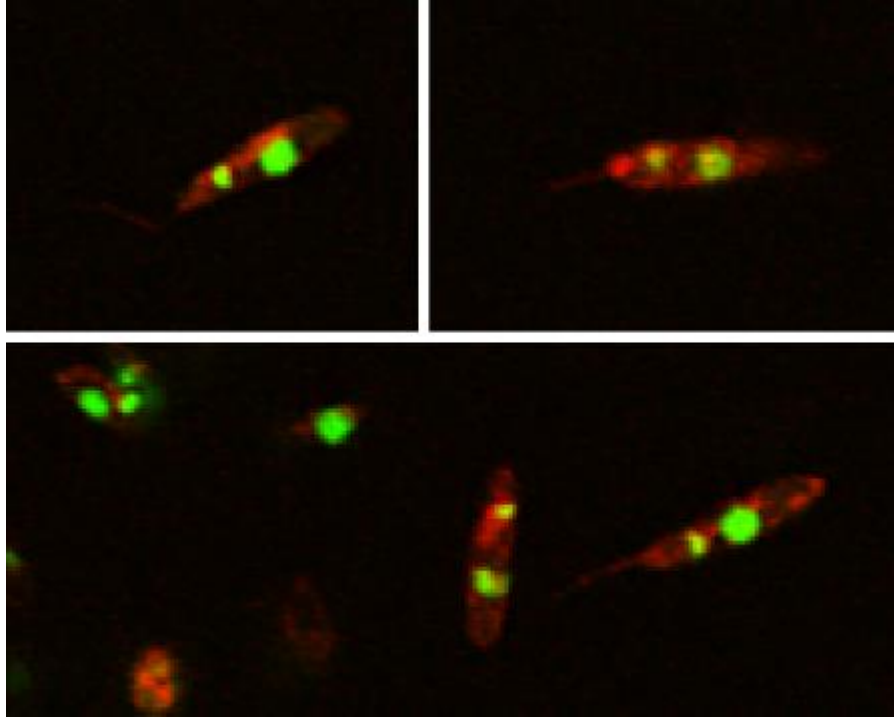


*Figure 32.* Visualization of CCT-mCherry by Confocal Microscopy. Overlay of *L. tarentolae* cells visualized in the green and red channels. The larger nucleus and smaller kinetoplast were labeled green by excitation of SYBR green using the blue Ar 488 nm laser. The CCT-mCherry fusion protein was labeled red by excitation of the mCherry tag with the green DPSS 561 nm laser.

Overlay of the ECT images showed no mixed fluorescence of the green and red channels, suggesting that the *L. major* ECT isoform did not localize to the nucleus or kinetoplast. ECT was shown to localize ubiquitously throughout the cytoplasm like the isoforms from mammals and *T. brucei* (Vermueulen et al., 1993; Gibellini et al., 2009) (Figure 33).

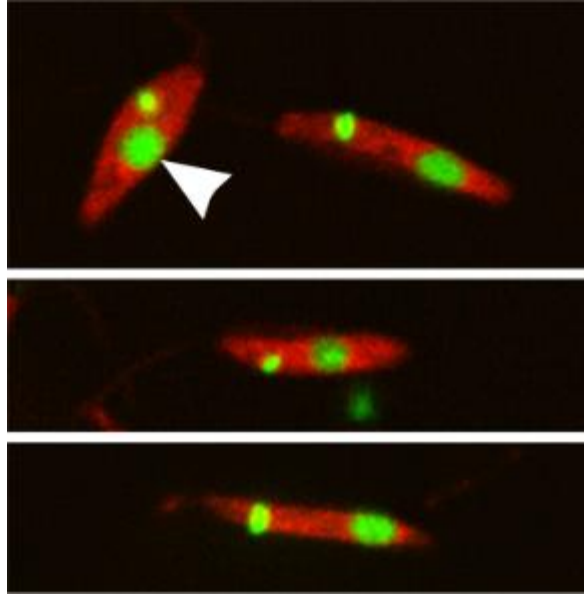


*Figure 33.* Visualization of ECT-mCherry by Confocal Microscopy. Overlay of *L. tarentolae* cells visualized in the green and red channels. The larger nucleus and smaller kinetoplast were labeled green by excitation of SYBR green using the blue Ar 488 nm laser. The ECT-mCherry fusion protein was labeled red by excitation of the mCherry tag with the green DPSS 561 nm laser.

## Conclusions and Future Work

Amino acid sequence analysis was used to identify the conserved cytidyltransferase catalytic motif in ECT, as well as a possible amino terminal membrane binding domain in CCT. The genes for CCT and ECT were also recombinantly expressed with mCherry red fluorescent protein (RFP) as a fusion protein construct in non pathogenic *L. tarentolae*. Visualization of the mCherry-tagged fusion proteins by confocal microscopy showed that CCT, like other isoforms from other organisms, was mostly cytoplasmic and possibly able to reversibly associate with internal membranes (Lykidis et al., 1998; Friesen, Park, and Kent, 2001; Tilley et al., 2008). This also revealed that ECT is completely cytoplasmic, as is the case with the isoforms of mammals and another parasite, *T. brucei* (Vermueulen et al., 1993; Gibellini et al., 2009).

Recombinant DNA encoding CCT from *L. major* was cloned from genomic DNA and the protein was produced by inducible expression in cells containing cold-adapted chaperonin proteins. Purification of the protein was accomplished using metal affinity column chromatography and a novel series of washes and incubations with ATP. Purified truncated CCT enzyme was then used to assay varying concentrations of CTP and [<sup>14</sup>C] PoC and determined the  $V_{max}$  to be approximately 374 nmol/mg/min, which was very close to that of another intracellular parasite, *P. falciparum*, but two to three orders of magnitude lower compared to those reported for full length isoforms from other organisms. The  $K_m$  for CTP and PoC was found to be 0.0648 mM and 3.74 mM respectively. These seemingly extreme values for  $K_m$  of both substrates of the enzyme from *L. major* compared to isoforms from other organisms may be explained by a difference of substrate concentration and availability within the macrophage host cell

(Friesen et al., 1999; Tilley et al., 2008; Helmink and Friesen, 2004; Friesen, Liu, and Kent, 2001; Friesen, Park, and Kent, 2001; Yeo et al., 1997). The  $Mg^{2+}$  ion was used as a cofactor in the reaction, but the enzyme was also able to achieve nearly maximal activity using  $Mn^{2+}$ ,  $Co^{2+}$ ,  $Ni^{2+}$ , and possibly  $Fe^{2+}$ . Additionally, the enzyme was most active at 37°C and pH 7.5.

The results obtained in this study used established experimental methods and were influenced by laboratory capabilities. As previously stated, this included the use of a truncated form of CCT in enzyme assays presumably because the amino terminal portion of the protein could not be produced in a bacterial expression system, most likely due to its hydrophobic nature. Therefore, future experiments should primarily be concerned with the cloning and production of full length CCT in a suitable, inducible expression system, such as the yeasts *S. cerevisiae* and *P. pastoris* or mammalian Chinese hamster ovary (CHO) cells. Assay of the full length CCT enzyme may yield more accurate kinetic parameters for the enzyme and its substrates, as well as provide a more representative influence of divalent metal cations, temperature, and pH on enzyme activity. This would also allow exploration of the effect of anionic lipids on activity, as their ability to induce conformational change by mimicking membrane binding plays a central role in other CCT isoforms (Friesen et al., 1999; Friesen, Liu, and Kent, 2001; Friesen, Park, and Kent, 2001).

Also, subjecting the amino-terminal region of the full protein to BLAST analysis reveals an interesting result. After the initial match to cytidylyltransferases from other species of *Leishmania*, the next highest BLAST score is attributed to several putative choline phosphotransferase (CPT) sequences, the third enzyme of the Kennedy pathway.



The CPT enzymes to which the amino-terminal region has similarity are from another protozoan, *Entamoeba histolytica*. Similarity was also indicated for a putative ethanolamine phosphotransferase (EPT) sequence from the mosquito *Aedes aegypti*, the analogous enzyme of PE synthesis. This presents an intriguing hypothesis of a dual function enzyme in *Leishmania* that catalyzes both the CCT and CPT reactions, directly synthesizing phosphatidylcholine from CTP, phosphocholine, and diacylglycerol species. Thus, the full length enzyme could be tested for CPT activity by adding diacylglycerol in 0.1% taurocholate to the standard CCT enzyme assay mixture and looking for PC synthesis (Sleight and Kent, 1980).

Next, the improvement of all biochemical characterization and kinetics studies should be paramount. This would mean the development of a new method to measure product formation from enzyme assays instead of radioisotope scintillation counting. This method is less accurate and reproducible than others because it measures the amount of product formed indirectly; by binding, washing, and releasing from charcoal. This has traditionally been the only method used to measure the amount of CDP-choline produced in a CCT assay because of the similarity in structure between CTP and CDP-choline. However, very recent development of liquid chromatography- tandem mass spectrometry (LC-MS/MS) has shown the ability to separate the substrate CTP and product CDP-choline using novel gradients of ammonium acetate and acetonitrile (Bapiro et al., 2014; Bapiro et al., 2011). LC-MS/MS would provide a method to directly measure product formation, providing more accurate data with less background. While an improvement for all experiments, this would be especially helpful in determining whether the effect of  $Fe^{2+}$  on *L. major* CCT was credible or if this particular cation caused an error in product

measurement. If the former is true, this could lead to a whole new view of the use of iron to regulate growth and infectivity in *Leishmania*.

Finally, CCT is an attractive potential drug target for leishmaniasis due its regulatory activity in the *de novo* synthesis of PC in the Kennedy pathway. This is strengthened by the hypothesis that the Kennedy pathway may be the predominant route for PC synthesis in infective amastigotes, as PEMT activity in these cells is nearly non-existent and the *Leishmania* cell would have a wealth of access to choline within the mammalian host (Bibis et al., 2014). The results concerning the biochemical properties of the enzyme from *L. major* are the first step of understanding how CCT functions in *Leishmania* cells. However, future studies should be primarily focused on expression and activity of CCT in the amastigote form; in a time course following its intracellular, bloodstream, and tissue-invasive stages. These experiments would require *L. major* amastigotes cultured from infected mice and the cell lysate supernatant would be used to measure enzyme activity. Measurement of expression would also require the raising of specific anti-CCT primary antibodies to use in Western blot immunoassay. Ultimately, results from these experiments would be compared with the data concerning PEMT in *L. major* amastigotes in order to clarify the value of CCT as a potential target in the treatment of leishmaniasis.



## REFERENCES

- Aktas, M., Wessel, M., Hacker, S., Klusener, S., Gleichenhagen, J., & Narberhaus, F. (2010). Phosphatidylcholine biosynthesis and its significance in bacteria interacting with eukaryotic cells. *Eur. J. Cell Biol.*, *89*, 888-894.
- Bapiro, T. E., Frese, K. K., Courtin, A., Bramhall, J. L., Madhu, B., Cook, N., Neesse, A., Griffiths, J. R., Tuveson, D. A., Jodrell, D. I., & Richards, F. M. (2014). Gemcitabine diphosphate choline is a major metabolite linked to the Kennedy pathway in pancreatic cancer models *in vivo*. *Br. J. Cancer*, *111*, 318-325.
- Bapiro, T. E., Richards, F. M., Goldgraben, M. A., Olive, K. P., Madhu, B., Frese, K. K., Cook, N., Jacobetz, M. A., Smith, D., Tuveson, D. A., Griffiths, J. R., & Jodrell, D. I. (2011). A novel method for quantification of gemcitabine and its metabolites 2',2'-difluorodeoxyuridine and gemcitabine triphosphate in tumor tissue by LC-MS/MS: comparison with <sup>19</sup>F NMR spectroscopy. *Cancer Chemother. Pharmacol.*, *68*, 1243-1253.
- Barnett, R. L., Ruffini, L., Ramsammy, L., Pasmantier, R., Friedlaender, M. M., & Nord, E. P. (1993). Angiotensin-mediated phosphatidylcholine hydrolysis and protein kinase C activation in mesangial cells. *Am. J. Physiol.*, *265*, 1100-1108.
- Bibis, S. S., Dahlstrom, K., Zhu, T., & Zufferey, R. (2014). Characterization of *Leishmania major* phosphatidylethanolamine methyltransferases *LmjPEM1* and *LmjPEM2* and their inhibition by choline analogs. *Mol. Biochem. Parasitol.*, *196*, 90-99.
- Bladergroen, B. A., Houweling, M., Geelen, M. J. H., & van Golde, L. M. G. (1999). Cloning and expression of CTP: phosphoethanolamine cytidyltransferase cDNA from rat liver. *Biochem. J.*, *343*, 107-114.
- Bradford, M. M. (1976). A rapid and sensitive method for the quantitation of microgram quantities of protein utilizing the principle of protein-dye binding. *Anal. Biochem.*, *72*, 248-254.
- Braker, J. D., Hodel, K. J., Mullins, D. R., & Friesen, J. A. (2009). Identification of hydrophobic amino acids required for lipid activation of *C. elegans* CTP: phosphocholine cytidyltransferase. *Arch. Biochem. Biophys.*, *492*, 10-16.
- Center for Disease Control (CDC). Parasites. Leishmania. <http://www.cdc.gov/parasites/leishmaniasis/> (accessed May 16, 2015).

- Coppolino, M. G., Dierckman, R., Loijens, J., Collins, R. F., Pouladi, M., Jongstra-Bilen, J., Schreiber, A. D., Trimble, W. S., Anderson, R., & Grinstein, S. (2002). Inhibition of phosphatidylinositol-4-phosphate 5-kinase I alpha impairs localized actin remodeling and suppresses phagocytosis. *J. Biol. Chem.*, *277*, 43849-43857.
- Ding, Z., Taneva, S. G., Huang, H. K., Campbell, S. A., Semenc, L., Chen, N., & Cornell, R. B. (2012). A 22-mer segment in the structurally pliable regulatory domain of metazoan CTP: phosphocholine cytidyltransferase facilitates both silencing and activating functions. *J. Biol. Chem.*, *287*, 38980-38991.
- Ferrer, M., Lunsdorf, H., Chernikova, T. N., Yakimov, M., Timmis, K. N., & Golyshin, P. N. (2004). Functional consequences of single:double ring transitions in chaperonins: life in the cold. *Mol. Microbiol.*, *53*, 167-182.
- Fong, D., Yim, V., D'Elia, M., Brown, E., & Berghuis, A. (2006). Crystal structure of CTP: glycerol-3-phosphate cytidyltransferase from *Staphylococcus aureus*: examination of structural basis for kinetic mechanism. *Biochim. Biophys. Acta*, *1764*, 63-69.
- Friesen, J. A., Campbell, H. A., & Kent, C. (1999). Enzymatic and cellular characterization of a catalytic fragment of CTP: phosphocholine cytidyltransferase alpha. *J. Biol. Chem.*, *274*, 13384-13389.
- Friesen, J. A., Liu, M. F., & Kent, C. (2001). Cloning and characterization of lipid-activated CTP: phosphocholine cytidyltransferase from *Caenorhabditis elegans*: identification of a 21-residue segment critical for lipid activation. *Biochim. Biophys. Acta.*, *1533*, 86-98.
- Friesen, J. A., Park, Y. S., & Kent, C. (2001). Purification and kinetic characterization of CTP: phosphocholine cytidyltransferase from *Saccharomyces cerevisiae*. *Protein Express. Purif.*, *21*, 141-148.
- Gibellini, F., Hunter, W. N., & Smith, T. K. (2009). The ethanolamine branch of the Kennedy pathway is essential in the bloodstream form of *Trypanosoma brucei*. *Mol. Microbiol.*, *73*, 826-843.
- Gibellini, F., & Smith, T. K. (2010). The Kennedy pathway: de novo synthesis of phosphatidylethanolamine and phosphatidylcholine. *IUBMB Life*, *62*, 414-428.
- Glaser, T. A., Utz, G. L., & Mukkada, A. J. (1992). The plasma membrane electrical gradient (membrane potential) in *Leishmania donovani* promastigotes and amastigotes. *Mol. Biochem. Parasitol.*, *51*, 9-15.

- Helmink, B. A., Braker, J., Kent, C., & Friesen, J. (2003). Identification of lysine 122 and arginine 196 as important functional residues of rat CTP: phosphocholine cytidyltransferase alpha. *Biochemistry*, *42*, 5043-5051.
- Helmink, B. A., & Friesen, J. A. (2004). Characterization of a lipid activated CTP: phosphocholine cytidyltransferase from *Drosophila melanogaster*. *Biochem. Biophys. Acta.*, *1683*, 78-88.
- Huynh, C., Sacks, D. L., & Andrews, N. W. (2006). A *Leishmania amazonensis* ZIP family iron transporter is essential for parasite replication within macrophage phagolysosomes. *J. Exp. Med.*, *203*, 2363-2375.
- Kalmar, G. B., Kay, R. J., LaChance, A. C., & Cornell, R. B. (1994). Primary structure and expression of a human CTP: phosphocholine cytidyltransferase. *Biochim. Biophys. Acta.*, *1219*, 328-334.
- Kaneko, H., Hosohara, M., Tanaka, M., & Itoh, T. (1976). Lipid composition of 30 species of yeast. *Lipids.*, *11*, 837-844.
- Kennedy, E. P., & Weiss, S. B. (1956). The function of cytidine coenzymes in the biosynthesis of phospholipids. *J. Biol. Chem.*, *222*, 193-214.
- Kent, C. (1997). CTP: phosphocholine cytidyltransferase. *Biochim. Biophys. Acta.*, *1348*, 79-90.
- Larvor, M. P., Cerdan, R., Gumila, C., Maurin, L., Seta, P., Roustan, C., & Vial, H. (2003). Characterization of the lipid-binding domain of the *Plasmodium falciparum* CTP: phosphocholine cytidyltransferase through synthetic-peptide studies. *Biochem. J.*, *375*, 653-661.
- Lee, J., Johnson, J., Ding, Z., Paetzel, M., & Cornell, R. B. (2009). Crystal structure of a mammalian CTP: phosphocholine cytidyltransferase catalytic domain reveals novel active site residues within a highly conserved nucleotidyltransferase fold. *J. Biol. Chem.*, *284*, 33535-33548.
- Lykidis, A., Murti, K. G., & Jackowski, S. (1998). Cloning and characterization of a second human CTP: phosphocholine cytidyltransferase. *J. Biol. Chem.*, *273*, 14022-14029.
- Miessler, G. L., & Tarr, D. A. (2004). *Inorganic Chemistry*, 3<sup>rd</sup> Ed. Singapore: Pearson Education.
- Morganthaler, A. N. (2014). Cloning of the gene encoding CTP: phosphoethanolamine cytidyltransferase and from *Leishmania major* and investigation of kinetic properties (unpublished masters thesis). Illinois State University, Normal IL.

- Murphy, E. J., Joseph, L., Stephens, R., & Horrocks, L. A. (1992). Phospholipid composition of cultured human endothelial cells. *Lipids.*, 27, 150-153.
- Park, Y. S., Gee, P., Sanker, S., Schurter, E.J., Zuiderweg, E. R. P., & Kent, C. (1997). Identification of functional conserved residues of CTP: glycerol-3-phosphate cytidyltransferase. *J. Biol. Chem.*, 272, 15161-15166.
- Park, Y. S., Sweitzer, T., Dixon, J., & Kent, C. (1993). Expression, purification, and characterization of CTP: glycerol-3-phosphate cytidyltransferase from *Bacillus subtilis*. *J. Biol. Chem.*, 268, 16648-16654.
- Patridge, K., Weber, C., Friesen, J. A., Sanker, S., Kent, C., & Ludwig, M. (2003). Glycerol-3-phosphate cytidyltransferase. Structural changes induced by binding of CDP-glycerol and the role of lysine residues in catalysis. *J. Biol. Chem.*, 278, 57863-57871.
- Rogers, M. B., Hilley, J. D., Dickens, N. J., Wilkes, J., Bates, P. A., Depledge, D. P., Harris, D., Her, Y., Herzyk, P., Imamura, H., Otto, T. D., Sanders, M., Seeger, K., Dujardin, J. C., Berriman, M., Smith, D. F., Hertz-Fowler, C. & Mottram, J. C. (2011). Chromosome and gene copy number variation allow major structural change between species and strains of *Leishmania*. *Genome Res.*, 21, 2129-2142.
- Schuiki, I., & Daum G. (2009). Phosphatidylserine decarboxylases, key enzymes of lipid metabolism. *IUBMB Life*, 61, 151-162.
- Singh, S., & Sivakumar, R. (2004). Challenges and new discoveries in the treatment of leishmaniasis. *J. Infect. Dis.*, 10, 307-315.
- Sleight, R., & Kent, C. (1980). Regulation of phosphatidylcholine in cultured chick embryonic muscle treated with phospholipase C. *J. Biol. Chem.*, 255, 10644-10650.
- Tilley, D. M., Evans, C. R., Larson, T. M., Edwards, K. A., & Friesen, J. A. (2008). Identification and characterization of the nuclear isoform of *Drosophila melanogaster* CTP: Phosphocholine Cytidyltransferase. *Biochemistry*, 47, 11838-11846.
- Vance, D. E. (2014). Phospholipid methylation in mammals: from biochemistry to physiological function. *Biochim. Biophys. Acta.*, 1838, 1477-1487.
- Vannier-Santos, M. A., Martiny, A., & de Souza, W. (2002). Cell biology of *Leishmania* spp.: invading and evading. *Curr. Pharm. Des.*, 8, 297-318.

- Vermueulen, P., Tijburg, L., Geelen, M., & van Golde, L. (1993). Immunological characterization, lipid dependence, and subcellular localization of CTP: phosphoethanolamine cytidyltransferase purified from rat liver. *J. Biol. Chem.*, 268, 7458-7464.
- Wanderley, J. L., Moreira, M. E., Benjamin, A., Bonomo, A. C., & Barcinski, M. A. (2006). Mimicry of apoptotic cells by exposing phosphatidylserine participates in the establishment of amastigotes of *Leishmania (L.) amazonensis* in mammalian hosts. *J. Immunol.*, 176, 1834-1839.
- Wang, Y., MacDonald, J. I. S., & Kent, C. (1995). Identification of the nuclear localization signal of rat liver CTP: phosphocholine cytidyltransferase. *J. Biol. Chem.*, 270, 354-360.
- Wang, X. M., & Moore, T. S. (1991). Phosphatidylethanolamine synthesis by castor bean endosperm. Intracellular distribution and characteristics of CTP: ethanolaminephosphate cytidyltransferase. *J. Biol. Chem.*, 266, 19981-19987.
- Weber, C., Park, Y. S., Sanker, S., Kent, C., & Ludwig, M. (1999). A prototypical cytidyltransferase: CTP: glycerol-3-phosphate cytidyltransferase from *Bacillus subtilis*. *Structure*, 7, 1113-1124.
- World Health Organization. Leishmaniasis. The Disease and its Epidemiology. [http://www.who.int/leishmaniasis/disease\\_epidemiology/en/](http://www.who.int/leishmaniasis/disease_epidemiology/en/) (accessed May 16, 2015).
- Yang, W., Mason, C. B., Pollock, S. V., Lavezzi, T., Moroney, J. V., & Moore, T. S. (2004). Membrane lipid biosynthesis *Chlamydomonas reinhardtii*: expression and characterization of CTP: phosphoethanolamine cytidyltransferase. *Biochem. J.*, 382, 51-57.
- Yeo, H. J., Larvor, M. P., Ancelin, M. L., & Vial, H. J. (1997). *Plasmodium falciparum* CTP: phosphocholine cytidyltransferase expressed in *Escherichia coli*: purification, characterization and lipid regulation. *Biochem. J.*, 324, 903-910.
- Zhang, K., & Beverly, S. M. (2009). Phospholipid and sphingolipid metabolism in *Leishmania*. *Mol. Biochem. Parasitol.*, 170, 55-64.
- Zhang, K., Pompey, J. M., Hsu, F., Key, P., Bandhuvula, P., Saba, J. D., Turk, J., & Beverly, S. M. (2007). Redirection of sphingolipid metabolism toward *de novo* synthesis of ethanolamine in *Leishmania*. *EMBO J.*, 26, 1094-1104.
- Zilberstein, D., & Shapira, M. (1994). The role of pH and temperature in the development of *Leishmania* parasites. *Annu. Rev. Microbiol.*, 48, 449-470.



Zufferey, R., Allen, S., Barron, T., Sullivan, D. R., Denny, P. W., Almeida, I. C., Smith, D. F., Turco, S. J., Ferguson, M. A., & Beverley, S. M. (2003). Ether phospholipids and glycosylinositolphospholipids are not required for amastigote virulence or for inhibition of macrophage activation by *Leishmania major*. *J. Biol. Chem.*, 278, 44708-44718.